

Licenciate

Kajsa-My Blomdahl

Mars 2019

Contents

1	Introduction	2
1.1	Background	2
1.2	The Birth of Efimov Physics	3
1.3	Theoretical Introduction	3
1.3.1	Entering the quantum realm	3
1.3.2	Two-body Interactions	4
1.3.3	Universality	5
2	Experimental Evidence	8
2.1	Efimov Trimers in Atomic Systems	8
2.2	Efimov States in Nuclei	8
2.3	Four-body Recombination connected to Efimov Trimers	8
3	Scattering Theory	8
3.1	Two-body Scattering	8
3.2	The low energy limit	13
3.3	Zero-Energy Scattering	14
4	The Three-body Problem	16
4.1	Mass Normalized Jacobi Coordinates	16
4.2	The Hyperspherical Method	19
4.2.1	Delves Coordinates	19
4.2.2	Smith-Whitten Coordinates	23
4.2.3	Symmetries	32
4.3	Adiabatic hyperspherical method	34
4.4	Generalized Hellmann-Feynman theorem	36
5	Numerical Approach	38
5.1	Basis splines expansion	38
5.2	Gauss-Legendre Quadrature	39
6	Results	39

1 Introduction

1.1 Background

The n -body problem is a class of problems in physics that, in a highly general sense, consists of modelling the motion of n objects interacting through some physical force. In classical mechanics the equations of motion for n point particles can be derived from Newton's second law of motion, which states that the rate of change in momentum for an object equals the force acting on it, or from analytical formulations such as Lagrangian and Hamiltonian mechanics, which consider scalar properties of motion like kinetic and potential energies. In the quantum regime, where the wave-like property of matter has to be taken into account, the state of an n -body system is described by a total wave function, where the Hamiltonian operator generates the time evolution of the state as given by Schrödinger's differential equation.

The core of the n -body problem is that neither the classical equations of motion nor the Schrödinger equation are analytically solvable for more than two interacting particles. Consider the case where $n = 3$. Although apparently simple, the configuration space for the three-body problem is six dimensional after separating out the center of mass motion. Three additional constants of motion can be provided by conservation of the total angular momentum, which effectively reduces the problem to that of three coupled second order non-linear differential equations in the classical case and a three dimensional Schrödinger equation in the quantum case.

The quest for a general solution to the classical three-body problem is renowned. As a recurrent muse to a number of great mathematicians during the past centuries, dating back to Newton himself, the three-body problem has been a catalyst for the development of analysis and the modern theory of dynamical systems [3]. Although there are a number of special cases that have explicit solutions, non-linear dynamical systems often display highly unpredictable behaviour due to sensitive dependencies on initial conditions, i.e. are chaotic. Nowadays, different numerical approaches are used to solve these kinds of problems, but the computational load can be substantial.

In contrast to the classical case, the quantum three-body problem is amenable to qualitative analysis [5] and in some cases, even to analytic solutions. In the quantum realm of few-body systems the Faddeev and the Faddeev-Yakubovsky equations, which are equivalent formulations of the Schrödinger equation for three- and four-body systems respectively, can, for a few special cases, be solved analytically by iteration [7, 17]. For the three-body scattering problem bound state solutions can exist in cases where all three two-body subsystems have short-ranged interactions, if at least two of these interactions are close to resonance. This is called the Efimov effect.

1.2 The Birth of Efimov Physics

In low energy scattering, particles are said to resonate when the strength of the attractive interaction between them barely cancels out the repulsive effect of the kinetic energy. During the collision they remain close for an extended period of time, in an almost bound state, before separating.

In 1970, Vitaly Efimov predicted that resonant two-body forces could give rise to a series of bound energy levels in three-particle systems [4]. When the short-ranged two-body forces approached resonance, he found a universal long-range three-body attraction emerging, giving rise to an infinite number of trimer states with binding energies obeying a discrete scaling law at resonance.

Efimov proposed that attractive three-body interaction appearing in systems with resonant short-ranged interactions and repulsive Coulomb forces could explain the binding of three particle nuclei such as the three nucleon triton ${}^3\text{H}$ and the triple-alpha Hoyle state of ${}^{12}\text{C}$.

The notion of Efimov physics comprises a range of universal phenomena that occur in few-body systems exhibiting the Efimov effect. Short-ranged forces commonly occur in nature and few-body effects are expected to appear in a broad range of physical systems. Development in the theory of few-body quantum systems is important since it could bridge the gap between existing well developed models of treating one- and two-body systems and the statistical methods used to describe many-body systems.

1.3 Theoretical Introduction

A short review concerning some important aspects of quantum mechanical systems and two-body scattering, in particular the concept of *scattering length*, will follow in order to set the stage for a discussion of quantum effects in few-body systems in general and Efimov states in three-body systems in particular.

1.3.1 Entering the quantum realm

All particles of matter exhibit wave-like properties. The wavelength of a particle with momentum p is given by the de Broglie equation

$$\lambda = \frac{h}{p} = \frac{h}{mv} \quad (1.1)$$

where h is the Planck constant. The wave characteristics of matter grow with increasing de Broglie wavelength. When the wavelength is sufficiently large, classical physics no longer applies and the system has reached the quantum regime. From 1.1 it is evident that this is true for particles that are very small or very slow. In an ultracold quantum gas, the atoms are cooled down to a point where they move so slowly that the increased uncertainty in position for the individual atoms becomes so large that they start to overlap with each other. At this point the atoms cannot be viewed as individual particles but as a correlated wave. The de Broglie wavelength of the atoms is then larger than the average

interatomic spacing, which is about one micron in a low density gas, and their behaviour are fully governed by quantum mechanics. In other words, the transition to the quantum regime occurs when the thermal de Broglie wavelength is on the order of the interparticle spacing. Since the temperature of the gas and the thermal de Broglie wavelength are related through

$$\lambda = \frac{h}{\sqrt{2\pi m k_B T}}, \quad (1.2)$$

in which k_B is the Boltzmann constant, it means there is a critical temperature for when the quantum effects become dominant. For a dilute atomic gas this critical temperature is in the microkelvin to nanokelvin range.

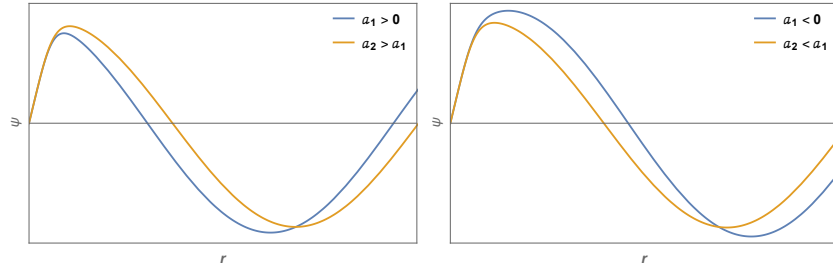
1.3.2 Two-body Interactions

Atomic interactions are pair-wise and short ranged, which means that they interact when they are close to each other. At sufficiently low energies, atoms behave like point particles and have quantized orbital angular momenta l . In analogy with electronic orbitals, the quantum numbers $l = 0, 1, 2$, associated with an atom are referred to as s -waves, p -waves, and d -waves respectively.

The scattering processes of two particles can be decomposed into that of an incoming plane wave – expanded into a sum of partial waves with definite angular momenta – which scatters off a potential placed at the origin. For low energy scattering, only the first few l -quantum numbers contribute to the scattering process and in the ultracold regime s -wave collisions dominate. Scattering becomes isotropic when the wavelength of the relative particle is much larger than the typical interparticle interaction range r_0 because the wave is then too large to resolve the details of the short-range interaction. In other words, the colliding atoms cannot resolve each other's internal structure provided by their electronic configurations. This makes scattering in the low energy limit indistinguishable from that of point particles. Furthermore, only spherical waves will come close enough to be scattered by the potential. Higher partial waves ($l > 0$) will not "feel" the potential since they will be reflected by a centrifugal barrier at separations greater than the interaction range. Two-body scattering in this regime is solely governed by a single parameter called the s -wave scattering length a . The s -wave scattering length, referred to as the scattering length from here on, is defined in the low-energy limit as

$$a = \lim_{k \rightarrow 0} -\frac{\tan \delta_0(k)}{k}, \quad (1.3)$$

where k is the wave number ($k = p/\hbar = \sqrt{2\mu E}/\hbar$) and $\delta_0(k)$ is the s -wave phase shift of the outgoing wave. For small k , the phase shift will behave as $\delta(k) \approx -ka + O(k^2)$. If scattering by a hard sphere is considered, the scattering length a is simply the radius of the sphere. In the low energy limit, the scattering properties for an arbitrary potential are the same as that of a hard sphere with radius a . Scattering can therefore occur at separations greater than the interaction range if the magnitude of the scattering length is sufficiently large.



(a) The wave function is pushed outwards when the magnitude of a positive scattering length is increased. (b) The wave is pulled inwards when the magnitude of a negative scattering length is increased.

Figure 1.1: Illustration of the phase shifts causing the effective interaction and how it depends on the sign and magnitude of a .

The scattering length characterizes the strength of the short-range interparticle interaction. Since a positive scattering length corresponds to a negative phase shift – which means the scattered wave is pushed out – the effective interaction will be repulsive and an increase in a will cause the underlying attractive potential in a two-body bound state to become less attractive. Increasing the magnitude of a negative scattering length will, on the other hand, make the potential more attractive since the phase shift is now positive and the scattered wave is pulled in, see fig. 1.1. Even though the effective interaction is attractive at negative scattering lengths, the interaction will always be too weak to support a two-body bound state.

In the absence of an interaction, the phase shift is simply zero. The strongest dephasing occurs when δ_0 takes the value $\pi/2 \pmod{\pi}$, whereupon two-body s-wave resonances are formed. This situation is of particular interest in this thesis because Efimov physics arises when the two-body interactions are near resonance. Since the phase shift for the s-wave can be written as $\delta_0 \propto -ka$ in the long wavelength limit ($k \ll r_0^{-1}$), it means that the scattering length a has to become much larger in magnitude than the interaction range r_0 for a two-body interaction to become resonant.

1.3.3 Universality

Particles with large scattering lengths – i.e. $|a| \gg r_0$ – in the low-energy regime have universal properties. The properties are universal in the sense that they depend on the scattering length alone and not on the details of the short-range interaction. For atoms interacting via short-ranged interactions the scattering length is considered large if its magnitude $|a|$ is much larger than the typical van der Waals length of the atomic species [2]. The van der Waals length is defined by

$$l_{vdW} = \left(\frac{2\mu C_6}{\hbar^2} \right)^{1/4}, \quad (1.4)$$

in which C_6 is the van der Waal coefficient of the r^{-6} term of the potential. For a system of two identical bosons with $a > 0$, there is a universal shallow two-body bound state near the scattering threshold, with binding energy

$$E_D = \frac{\hbar^2}{2\mu a^2}. \quad (1.5)$$

For $a < 0$ there is no such bound state. Outside the universal range the natural binding energy for two particles should be approximately $1/mr_0^2$. The cross section for elastic scattering of two identical bosons in this regime is also universal and so is the mean square radius, each given by

$$\sigma = 8\pi a^2 \quad (1.6)$$

and

$$\langle r^2 \rangle = \frac{a^2}{2}, \quad (1.7)$$

respectively. The universal quantities given in eqs. (1.5) to (1.7) are exact for $a = \pm\infty$ and approximate for $|a| \gg r_0$. The unique dependence on this one length parameter also leads to continuous scaling symmetries in these quantities. If the scattering length is scaled with some real factor λ such that $a \rightarrow \lambda a$, the shallow dimer energy will scale as

$$E_D(\lambda a) = \lambda^{-2} E_D(a), \quad (1.8)$$

while the elastic cross section and the mean square radius scale as

$$\sigma_e(\lambda^{-2}k, \lambda a) = \lambda^2 \sigma_e(k, a) \quad (1.9)$$

and

$$\langle r^2(\lambda a) \rangle = \lambda^2 \langle r^2(a) \rangle, \quad (1.10)$$

respectively.

While the scattering length completely governs the low energy two-body collision problem, it is also the main parameter for describing the interaction of particles at very low collision energies in general.

Similarly to the universal quantities found in the two-body sector, three-body systems can also exhibit universal properties. For particles interacting through short-ranged interactions near resonance – i.e. when the attraction are on the verge on, or can just barely support a shallow dimer – an effective long-range three-body attraction emerge, which can form shallow three-body bound states with binding energies E_T^n that scale geometrically in the trimer region, see fig. 1.2. To understand how this long-range interaction is formed, consider a

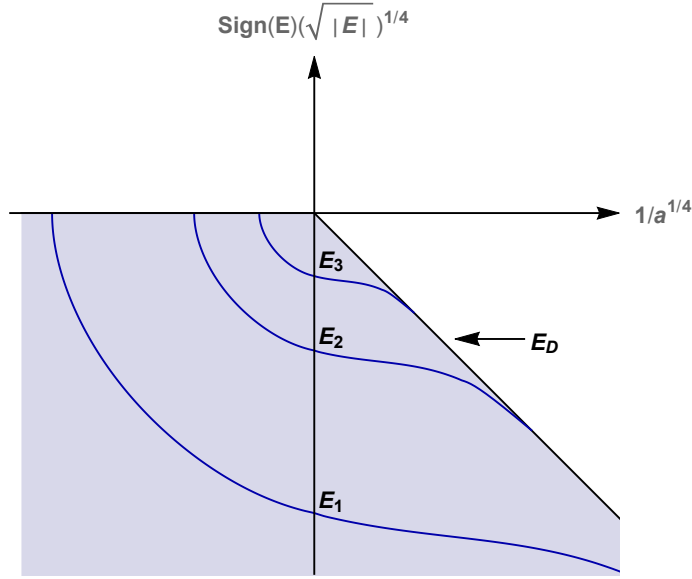


Figure 1.2: The energies of the three first Efimov states are plotted as a function of the inverse scattering length a . Three different regions can be identified in the figure. The three atom continuum is the region above the zero-energy threshold. The atom-dimer region is the region enclosed by the horizontal axis and the atom-dimer threshold and the trimer region shown in gray, in which Efimov states are represented by the blue lines.[1]

collision between the shallow dimer and a third particle in the low energy limit. The third particle will start to "feel" the dimer when it comes close to the two-body scattering length a , which is also the size of the dimer. At this point the third particle could tug off any of the particles in the dimer to form a new pair. It is this process of particle exchange which results in the effective three-body interaction that Vitaly Efimov found when he was studying the quantum three-body problem. This effective long-range attraction is universal in the sense that it emerges irrespective of the underlying two-body short-range interactions. The scaling in this sector is discrete. The infinite ladder of energy levels that appear in the asymptotic limit when $a \rightarrow \pm\infty$ have a discrete geometric scaling symmetry. The size of an excited state is larger than the previous state by a factor of $\lambda = e^{\pi/s_0} \simeq 22.7$. The scaling law applies radially see figure bla bla

$$\frac{E_T^{n+1}}{E_T^n} = e^{2\pi/s_0} \quad (1.11)$$

$$N \approx \pi^{-1} \ln(|a|/r_0) \quad (1.12)$$

2 Experimental Evidence

2.1 Efimov Trimers in Atomic Systems

Ultracold atomic clouds provided the first staging ground for exploring Efimov physics and related few-body phenomena because of the ability to control atom-atom interactions by an external field. In these extremely dilute gases, with densities n , the probability for collisions can reach unity by tuning the s-wave scattering length to the unitary regime $n|a^3| \gg 1$. In experiments with trapped ultracold atomic and molecular gases of alkali atoms with tunable two-body interactions, the existence of Efimov trimers have been inferred from resonantly enhanced loss rates, either in atomic three-body recombination processes at negative a , when the Efimov state couples to the triatomic threshold, or in atom-dimer relaxation processes.

Alkali atomic gases The first observations of an Efimov state was in an ultracold gas of ^{133}Cs was reported in 2006 by the group of Grimm and coworkers [11]. Later experiments have strengthen the evidence of these elusive states and in 2014 observations of the first excited Efimov state confirmed the theoretically predicted universal scaling properties of two successive Efimov states [9]. Efimov resonances in homogenic gases with other atomic species have been observed including ^{85}Rb , ^{39}K , ^7Li , and three component fermi gases of ^6Li . Also mixtures of ^{41}K and ^{87}Rb has been investigated.

Helium trimers Helium is a prime candidate to study Efimov physics with a more direct approach. The ground state of the helium trimer is not an Efimov state. However the first and second excited trimer have Efimov characteristics. Coulomb explosion imaging of helium trimers have revealed the geometric form of the trimers. [12]

2.2 Efimov States in Nuclei

2.3 Four-body Recombination connected to Efimov Trimers

The Efimov scenario is even richer. In connection to an Efimov trimer, a pair of four-body states can form when a fourth atom approach. In accordance with the theoretical predictions, strong evidence for the existence of a pair of four-body states was provided in 2009 [8].

3 Scattering Theory

3.1 Two-body Scattering

A collision between a pair of particles can be described in their center-of-mass frame as the scattering of a particle with reduced mass μ ($\mu = m_1 m_2 / (m_1 +$

$m_2))$ by the potential $V(\mathbf{r})$. The time-independent Schrödinger equation for the relative motion is then given by

$$\left[-\frac{\hbar^2}{2\mu}\nabla^2 + V(\mathbf{r}) \right] \psi(\mathbf{r}) = \frac{\hbar^2 k^2}{2\mu} \psi(\mathbf{r}), \quad (3.1)$$

where \mathbf{r} denotes the interparticle separation and ∇^2 the Laplace operator, which in spherical coordinates reads

$$\nabla^2 = \frac{1}{r^2} \frac{\partial}{\partial r} \left(r^2 \frac{\partial}{\partial r} \right) + \frac{1}{r^2 \sin \theta} \frac{\partial}{\partial \theta} \left(\sin \theta \frac{\partial}{\partial \theta} \right) + \frac{1}{r^2 \sin^2 \theta} \frac{\partial^2}{\partial \phi^2}. \quad (3.2)$$

By requiring the potential to be zero at large interparticle separation, the collision can be described as that of an incident plane wave with definite angular momentum that scatters off a potential placed at the origin. The potential will deflect some of the incident waves to form scattered waves, which at large distances will be diverging from a point source in the scattering region. Let r_0 denote the range of the action of the potential and let z denote the direction of the propagation of the incident plane wave. The boundary condition at large separations $r \gg r_0$ then imposes a solution of the following asymptotic form

$$\psi(\mathbf{r}) \xrightarrow{r \rightarrow \infty} e^{ikz} + f(k, \theta, \phi) \frac{e^{ikr}}{r}, \quad (3.3)$$

in which the total wave function is written as a superposition of the incident and scattered wave, with a scattering amplitude $f(k, \theta, \phi)$ that depends on the energy of the particle through k , the deflection angle θ between the waves and the azimuthal angle ϕ about the z -axis. For spherically symmetric potentials, i.e. $V(\mathbf{r}) = V(r)$, the Schrödinger equation (3.1) is separable. The incident and scattered wave functions are then conveniently expanded on a basis set of eigenfunctions of \mathbf{L}^2 and L_z , where \mathbf{L} is the relative orbital angular momentum operator. These eigenfunctions are the spherical harmonic functions $Y_l^m(\theta, \phi)$, which satisfy

$$\mathbf{L}^2 Y_l^m(\theta, \phi) \equiv -\frac{1}{\sin^2 \theta} \left[\sin \theta \frac{\partial}{\partial \theta} \left(\sin \theta \frac{\partial}{\partial \theta} \right) + \frac{\partial^2}{\partial \phi^2} \right] Y_l^m(\theta, \phi) = l(l+1) Y_l^m(\theta, \phi). \quad (3.4)$$

The most general solution to (3.1) is then of the form

$$\psi(\mathbf{r}) = \sum_{l=0}^{\infty} \sum_{m=-l}^l C_{lm} \frac{u_l(r)}{r} Y_l^m(\theta, \phi). \quad (3.5)$$

The separability of $\psi(\mathbf{r})$ effectively reduces the problem to that of solving the radial equation

$$\left[-\frac{d^2}{dr^2} + \frac{l(l+1)}{r^2} + \frac{2\mu}{\hbar^2} V(r) - k^2 \right] u_l(r) = 0. \quad (3.6)$$

By requiring the wave function to be finite everywhere it is implied that $u_l(r)$ must vanish at the origin. In the case where $V(r) = 0$, the solutions to the radial equation for positive energies have the form

$$u_l(r) \propto r j_l(kr), \quad (3.7)$$

where $j_l(kr)$ are the spherical Bessel functions. In the case of a non-zero potential the solutions need to be regular at the origin, while at large distances $r \gg r_0$ they have the form

$$u_l(r) = r(a_l j_l(kr) + b_l y_l(kr)), \quad (3.8)$$

where $y_l(kr)$ are the spherical Neumann functions. Asymptotically the solutions (3.8) behave like

$$u_l(r) \xrightarrow{r \rightarrow \infty} \frac{1}{k} (a_l \sin(kr - l\frac{\pi}{2}) - b_l \cos(kr - l\frac{\pi}{2})). \quad (3.9)$$

By defining the ratio of the coefficients as

$$\frac{b_l}{a_l} = -\tan \delta_l(k), \quad (3.10)$$

where $\delta_l(k)$ is an energy dependent phase shift, the normalized asymptotic radial solutions for a non-vanishing potential can be written

$$\begin{aligned} u_l(r) &\xrightarrow{r \rightarrow \infty} \frac{1}{k} \left(\sin(kr - l\frac{\pi}{2} + \delta_l(k)) \right) \\ &= \frac{e^{-i\delta_l(k)}}{2ik} \left((-1)^{l+1} e^{-ikr} + e^{2i\delta_l(k)} e^{ikr} \right). \end{aligned} \quad (3.11)$$

Since the incident plane wave (3.3) is aligned with the z -axis, it is an eigenfunction of L_z with eigenvalue $m = 0$. The plane wave expansion is thus independent of the azimuthal angle around the z -axis and can therefore be expressed as

$$e^{ikz} = \sum_{l=0}^{\infty} (2l+1) i^l j_l(kr) P_l(\cos \theta), \quad (3.12)$$

where $P_l(\cos \theta)$ are Legendre polynomials. It is evident that this plane wave is a solution to (3.1) for $V(r) = 0$. Asymptotically the solutions (3.12) behave like

$$e^{ikz} \xrightarrow{r \rightarrow \infty} \frac{1}{2ikr} \sum_{l=0}^{\infty} (2l+1) P_l(\cos \theta) \left((-1)^{l+1} e^{-ikr} + e^{ikr} \right). \quad (3.13)$$

The incident plane wave can thus be resolved into that of incoming (e^{-ikr}) and outgoing (e^{ikr}) spherical waves with a relative phase of 0 for l with odd parity and π otherwise. The scattering amplitude is Substituting (3.13) into (3.3) results in an asymptotic wave function of the form

$$\psi(\mathbf{r}) \xrightarrow{r \rightarrow \infty} \frac{1}{2ikr} \sum_{l=0}^{\infty} (2l+1) P_l(\cos \theta) ((-1)^{l+1} e^{-ikr} + e^{ikr}) + f(k, \theta) \frac{e^{ikr}}{r}, \quad (3.14)$$

where $f(k, \theta, \phi) = f(k, \theta)$ because the scattering potential is spherically symmetric. Since the system is rotationally invariant about the z -axis, the scattered wave function must be azimuthally symmetric, i.e. have magnetic quantum number $m = 0$, wherefore the general solution (3.5) becomes

$$\psi(\mathbf{r}) = \sum_{l=0}^{\infty} c_l \frac{u_l(r)}{r} P_l(\cos \theta), \quad (3.15)$$

in which c_l are unknown coefficients. The asymptotic behaviour of (3.15) is thus

$$\psi(\mathbf{r}) \xrightarrow{r \rightarrow \infty} \frac{1}{2ikr} \sum_{l=0}^{\infty} c_l P_l(\cos \theta) e^{-i\delta_l(k)} ((-1)^{l+1} e^{-ikr} + e^{2i\delta_l(k)} e^{ikr}). \quad (3.16)$$

By comparing the asymptotic form of the incoming waves expressed in eqs. (3.14) and (3.16) it is evident that the coefficients $c_l = (2l+1)e^{i\delta_l(k)}$. The asymptotic scattered wave is thus

$$\psi(\mathbf{r}) \xrightarrow{r \rightarrow \infty} \frac{1}{2ikr} \sum_{l=0}^{\infty} (2l+1) P_l(\cos \theta) ((-1)^{l+1} e^{-ikr} + e^{2i\delta_l(k)} e^{ikr}). \quad (3.17)$$

For elastic scattering the flux of incoming and outgoing waves is conserved. The presence of a scattering potential will modify the plane wave by changing the relative phase of the incoming and outgoing waves by a phase shift $\delta_l(k)$ for each partial wave with angular momentum l . The phase shift $\delta_l(k)$ is thus a measure of the distortion of $u_l(r)$ from the free solution due to the presence of a scattering potential. Depending on whether the potential is attractive or repulsive, the scattered wave will either be pulled in or pushed out, respectively, by the scatterer. The scattering amplitude $f(k, \theta)$ is determined by comparing the outgoing waves in eqs. (3.14) and (3.17), resulting in

$$f(k, \theta) = \sum_{l=0}^{\infty} (2l+1) f_l(k) P_l(\cos \theta), \quad (3.18)$$

where the partial amplitude f_l can be expressed in the following ways

$$f_l(k) = \frac{e^{2i\delta_l(k)} - 1}{2ik} = \frac{e^{i\delta_l(k)} \sin \delta_l(k)}{k} = \frac{1}{k \cot \delta_l(k) - ik}. \quad (3.19)$$

The differential and the total cross-sections are determined from the scattering amplitude through

$$\frac{d\sigma}{d\Omega} = |f(k, \theta)|^2, \quad (3.20)$$

and

$$\sigma(k) = \sum_{l=0}^{\infty} \sigma_l(k) = \frac{4\pi}{k^2} \sum_{l=0}^{\infty} (2l+1) \sin^2 \delta_l(k), \quad (3.21)$$

in which σ_l is the scattering cross-section for each partial wave. So far, we have assumed that the particles are distinguishable and that scattering in the direction θ could be discriminated from that of scattering in the direction $\pi - \theta$. However, for identical particles these collisional processes will lead to the same final state. Interchanging the spatial coordinates of the particles $\mathbf{r}_1 \leftrightarrow \mathbf{r}_2$ corresponds to replacing the relative position vector \mathbf{r} by $-\mathbf{r}$, which in polar coordinates corresponds to replacing (r, θ, ϕ) by $(r, \pi - \theta, \phi + \pi)$. Thus, to accurately describe scattering of identical particles the quantum statistics of the particles must be taken into account to assure that the wave function of the total system has the correct symmetry properties. The wave function given in (3.3) does not fulfill this requirement. Instead, the correct two-body wave function in the center-of-mass frame for indistinguishable particles is retrieved by symmetrization (bosons, $\epsilon = 1$) or antisymmetrization (fermions, $\epsilon = -1$), leading to

$$\psi(\mathbf{r}) \xrightarrow{r \rightarrow \infty} \frac{e^{ikz} + \epsilon e^{-ikz}}{\sqrt{2}} + \frac{f(k, \theta) + \epsilon f(k, (\pi - \theta))}{\sqrt{2}} \frac{e^{ikr}}{r}. \quad (3.22)$$

In classical mechanics, the differential cross-sections for the two processes described above would simply add up. However, the quantum mechanical differential cross-section for indistinguishable particles is given by

$$\frac{d\sigma}{d\Omega} = |f(k, \theta) + \epsilon f(k, (\pi - \theta))|^2, \quad \text{for } 0 \leq \theta \leq \frac{\pi}{2}, \quad (3.23)$$

where the sum of probability amplitudes is

$$f(k, \theta) \pm f(k, (\pi - \theta)) = \frac{1}{2ik} \sum_{l=0}^{\infty} [1 \pm (-1)^l] (2l+1) P_l(\cos \theta) (e^{2i\delta_l(k)} - 1). \quad (3.24)$$

Note that the total cross section is obtained by integrating over half of the solid angle $\Omega = 4\pi$ in the case of identical particles. The expression for the total cross section for elastic scattering after integration is then

$$\sigma(k) = \frac{8\pi}{k^2} \sum_{l=0}^{\infty} (2l+1) \sin^2 \delta_l(k). \quad (3.25)$$

In the case of bosons (fermions), only even (odd) values of l will contribute to the total cross section (3.25).

3.2 The low energy limit

At very low energies – i.e. when the angular de Broglie wavelength $\lambda = 1/k$ is much larger than the interparticle interaction range $kr_0 \ll 1$ – higher partial waves becomes unimportant except for potentials that are strong enough to form $l \neq 0$ bound states near threshold ($E \simeq 0$). This can be understood classically by considering that particles with angular momentum l and energies much lower than the height of the centrifugal barrier – i.e. the angular momentum term in the effective potential $V_{eff} = V(r) + \hbar^2 l(l+1)/2\mu r^2$ – will simply be reflected by the barrier and only the lowest partial wave $l = 0$ will be able to come close enough to be scattered by the potential $V(r)$. For short-ranged two-body interactions – i.e. potentials that fall off faster than r^{-2} – the angular momentum term is the potential of longest range and will thus largely govern the threshold behaviour ($E = 0$) of the radial wave function. Since the potential and the k^2 term can be neglected in the radial equation (3.6) for separations larger than the interaction range $r \gg r_0$, the general solution $R_l = u_l/r$ at threshold is given by

$$R_l(E = 0) = c_1 r^l + c_2 r^{-(l+1)}. \quad (3.26)$$

By joining this solution to the asymptotic solution for $E > 0$, given in (3.11) one can show that

$$\tan \delta_l(k) \simeq \delta_l(k) = \frac{c_2}{c_1} \frac{k^{2l+1}}{(2l-1)!!(2l+1)!!} = (-a_l k)^{2l+1}, \quad (3.27)$$

in which a_l is the scattering length for the l 'th partial wave. The arguments above form the basis of the Wigner threshold law [13, 14], which states that at near threshold, the phase shift goes to zero like

$$\delta_l(k) \propto k^{2l+1} \pmod{\pi} \quad \text{when } k \rightarrow 0. \quad (3.28)$$

The cross-section for that partial wave then approaches zero like

$$\sigma_{l \neq 0}(k) = \frac{8\pi}{k^2} (2l+1) \sin^2 \delta_l(k) \propto k^{4l} \quad \text{when } k \rightarrow 0, \quad (3.29)$$

wherefore s-wave scattering is dominant for short-ranged potentials in the low energy limit. The only non-zero cross-section is that for the s-wave, which using (3.19), is given by

$$\sigma = \sigma_0 = 8\pi \lim_{k \rightarrow 0} \left| \frac{1}{k \cot \delta_0 - ik} \right|^2 = 8\pi a^2, \quad (3.30)$$

in the case of identical bosons ($\sigma = 4\pi a^2$ for distinguishable particles) and where a is the s-wave scattering length, previously defined in (1.3).

3.3 Zero-Energy Scattering

In the ultracold regime the energy is extremely low and $k \simeq 0$. The radial equation simplifies to

$$-\frac{d^2 u_l(r)}{dr^2} + \frac{2\mu}{\hbar^2} V(r) u_l(r) = 0 \quad (3.31)$$

The asymptotic solution for $l = 0$ ($u = u_0$) is then

$$u(r) \xrightarrow{r \rightarrow \infty} \frac{1}{k} \sin \left[k \left(r + \frac{\delta_0}{k} \right) \right] \xrightarrow{k \rightarrow 0} \text{constant}(r - a). \quad (3.32)$$

The logarithmic derivative is given by

$$\frac{u'(r)}{u(r)} \xrightarrow{r \rightarrow \infty} k \cot \left[k \left(r + \frac{\delta_0}{k} \right) \right] \xrightarrow{k \rightarrow 0} \frac{1}{r - a}. \quad (3.33)$$

In the limit $kr \ll 1$, the scattering length is obtained as

$$a = - \lim_{k \rightarrow 0} \frac{\tan \delta_0}{k} = \lim_{k, r \rightarrow 0, \infty} \left(r - \frac{u(r)}{u'(r)} \right). \quad (3.34)$$

From equation (3.32) it is evident that the scattering length is simply the radius at which the tangent to the radial wave intercept the r -axis. This concept can be illustrated by using a short-ranged attractive model potential given by

$$V(r) = - \frac{c_w \left[1 - \left(1 + \frac{r^2}{r_c^2} \right) e^{-\frac{r^2}{r_c^2}} \right]}{r^6}, \quad (3.35)$$

in which r_c and c_w are tuning parameters for the distance to the nadir and the depth of the potential, respectively. The scattering length can be varied by fine-tuning the potential depth, see fig. 3.2. Starting with an attractive potential with negative scattering length, i.e. with a tangent intercept on the negative side, when increasing the potential depth, the magnitude of the scattering length will increase and as $a \rightarrow -\infty$ the radial wave function will become flat. A further increase in potential depth will cause a to change sign $a \rightarrow \infty$. The sign shift of a is associated with the forming of a bound state. After the change in sign, a further increase in depth will instead corresponds to decreasing a since the radial wave function now crosses the r -axis on the positive side, with the intercept subsequently approaching the origin, see fig. 3.1. This behavior is then repeated in the same way until a new bound state is formed, see fig. 3.3.

Positive scattering lengths thus correspond to repulsive effective interactions, which means that the interaction can appear repulsive even in the case of an underlying attractive two-body interaction.

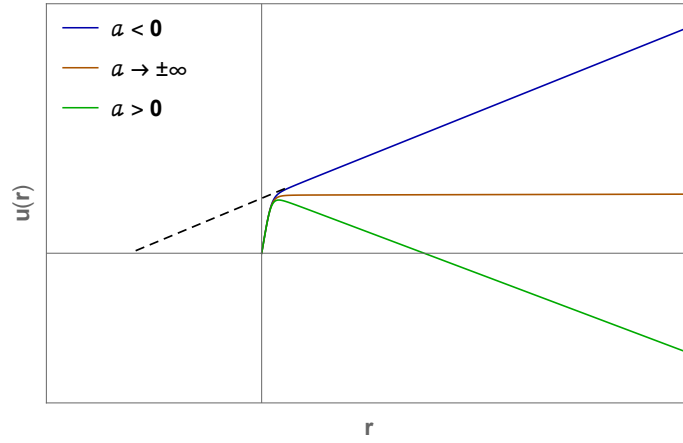


Figure 3.1: Plot of $u(r)$ versus r for the model potential (3.35) at three different depths. The radius at which the tangent intercept the r -axis gives the value of a .

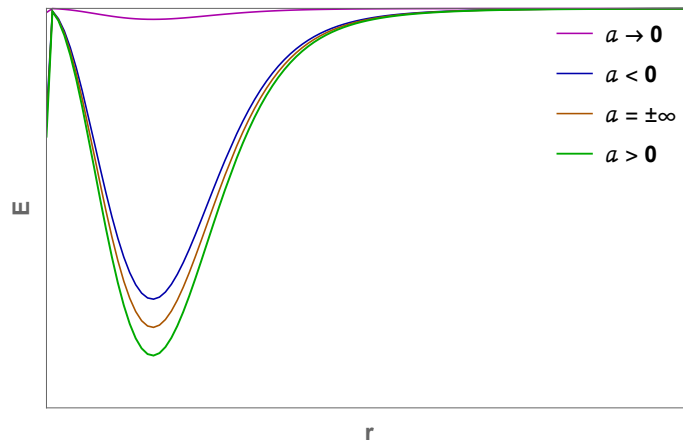


Figure 3.2: The three lowest curves correspond to the potentials used in fig. 3.1. As the magnitude of a negative a increases, the potential becomes more attractive until it reaches a constant depth at $a = \pm\infty$. After the change in sign, a further increase of a will instead have a repulsive effect on the interaction.

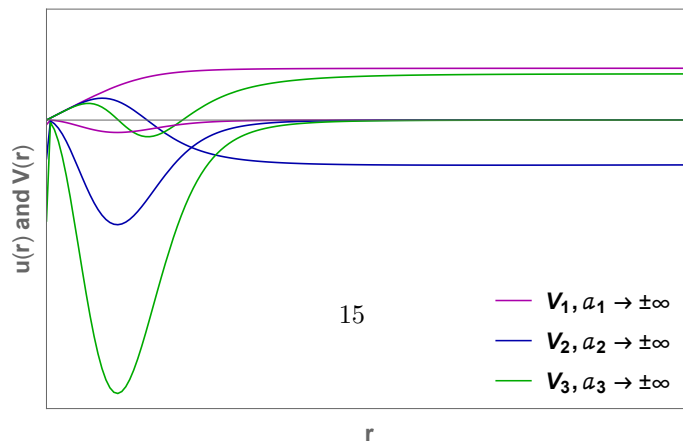


Figure 3.3: Illustration of three potentials and their corresponding radial wave functions

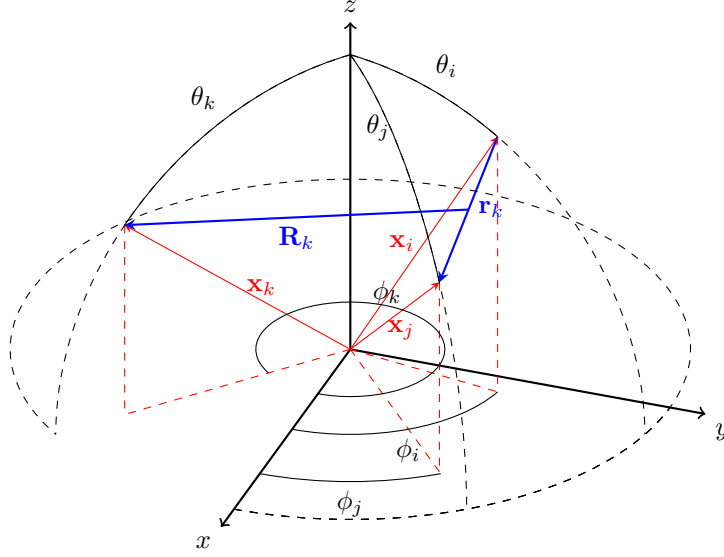


Figure 4.1: Spatial positions of three particles.

4 The Three-body Problem

Two-body scattering processes basically concern two different situations, elastic and inelastic collisions. For the three-body problem, solving the three-body Schrödinger equation is more involved. The enhanced complexity is mainly due to the increased number of fragmentation channels in the scattering processes. In addition to the triatomic fragmentation channel (1+1+1), there are three possible atom-dimer fragmentation channels (1+2). This makes the construction of permutation symmetric wavefunctions highly non trivial.

There are different routes of solving the three-body problem, it involves either solving the three-body Schrödinger equation or solving the Faddeev equation, which is equivalent to solving the three-body Schrödinger equation in configuration space. However, most approaches start with the same steps. This includes separating out the center of mass motion and then defining a set of relative coordinates. A convenient choice for the three-body problem is mass normalized Jacobi coordinates, since it removes the mass factors in the kinetic energy operator.

4.1 Mass Normalized Jacobi Coordinates

The spatial position of three particles in \mathbb{R}^3 are fixed by nine coordinates x_α^i , where $i(= 1, 2, 3)$ labels the particles, and $\alpha(= 1, 2, 3)$ their Cartesian space coordinates, respectively. Let \mathbf{x}_i and m_i be the position vector and mass of the i th particle in the laboratory frame. If the total mass M , the three particle reduced mass μ , and the normalizing constants d_k ($k = 1, 2, 3$) are given by

$$M = \sum_{i=1}^3 m_i, \quad (4.1)$$

$$\mu^2 = \prod_{i=1}^3 m_i / M, \quad (4.2)$$

$$d_k^2 = \frac{m_k}{\mu} \frac{(m_i + m_j)}{M}. \quad (4.3)$$

Then a set of mass scaled Jacobi coordinates and the center of mass coordinate can be defined as

$$\mathbf{r}_k = d_k^{-1}(\mathbf{x}_j - \mathbf{x}_i), \quad (4.4)$$

$$\mathbf{R}_k = d_k \left[\mathbf{x}_k - \frac{(m_i \mathbf{x}_i + m_j \mathbf{x}_j)}{m_i + m_j} \right], \quad (4.5)$$

$$\mathbf{X}_{CM} = \frac{1}{M} \sum_{i=1}^3 m_i \mathbf{x}_i. \quad (4.6)$$

In which, the indices i, j, k are cyclic permutations of $(1, 2, 3)$. Subsequently, the kinetic energy operator for the three particles in the laboratory frame, as given by

$$\hat{T} = -\frac{\hbar^2}{2} \sum_{i=1}^3 m_i^{-1} \nabla_{\mathbf{x}_i}^2, \quad (4.7)$$

will transform into

$$\hat{T} = -\frac{\hbar^2}{2\mu} \left(\nabla_{\mathbf{r}_k}^2 + \nabla_{\mathbf{R}_k}^2 \right) - \frac{\hbar^2}{2M} \nabla_{\mathbf{X}_{CM}}^2. \quad (4.8)$$

Now, since the interaction $V(\mathbf{r}_k, \mathbf{R}_k)$ do not depend on \mathbf{X}_{cm} , the center of mass motion decouples from the internal motion in the Schrödinger equation if we write the wavefunction as

$$\Psi(\mathbf{r}_k, \mathbf{R}_k, \mathbf{X}_{cm}) = \varphi(\mathbf{X}_{cm}) \psi(\mathbf{r}_k, \mathbf{R}_k), \quad (4.9)$$

so that

$$(H_{cm} + H_{int}) \varphi_k(\mathbf{X}_{cm}) \psi_n(\mathbf{r}_k, \mathbf{R}_k) = (E_k^{cm} + E_n^{int}) \varphi_k(\mathbf{X}_{cm}) \psi_n(\mathbf{r}_k, \mathbf{R}_k). \quad (4.10)$$

In the following text we will only consider the internal motion part of the Schrödinger equation. To clarify the notions in the following text, wavefunctions and energies labelled Ψ and E refers to the internal eigenstates and eigenenergies, which was labelled ψ and E^{int} previously.

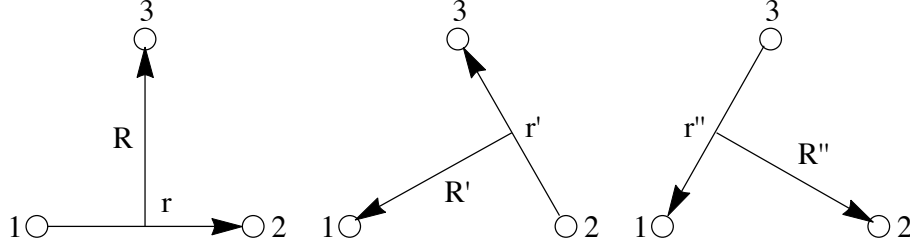


Figure 4.2: Three different Jacobi coordinates.

There are three possible ways to construct the Jacobi coordinates described above, see Figure 4.2. Each set transforms into one of the other by exchange of particles. For convenience, indices will often be suppressed in the following text, in these cases $(\mathbf{r}_k, \mathbf{r}_i, \mathbf{r}_j)$ correspond to $(\mathbf{r}, \mathbf{r}', \mathbf{r}'')$. Ignoring the mass scale factors in the coordinates we define the permutation operator for exchange of particles $(1 \rightarrow 3)$ as

$$\hat{P}_{13} = \begin{cases} \mathbf{r}' = \mathbf{x}_2 - \mathbf{x}_3 = \frac{1}{2}\mathbf{r} - \mathbf{R}, \\ \mathbf{R}' = \mathbf{x}_1 - \frac{1}{2}(\mathbf{x}_3 + \mathbf{x}_2) = -\frac{1}{2}(\frac{3}{2}\mathbf{r} + \mathbf{R}). \end{cases} \quad (4.11)$$

Similarly, the permutation operator for exchange of particles $(2 \rightarrow 3)$ are defined as

$$\hat{P}_{23} = \begin{cases} \mathbf{r}'' = \mathbf{x}_3 - \mathbf{x}_1 = \frac{1}{2}\mathbf{r} + \mathbf{R}, \\ \mathbf{R}'' = \mathbf{x}_2 - \frac{1}{2}(\mathbf{x}_1 + \mathbf{x}_3) = -\frac{1}{2}(\frac{3}{2}\mathbf{r} - \mathbf{R}). \end{cases} \quad (4.12)$$

For describing permutations in a system with mass-scaled coordinates it is useful to introduce angles defined by the particle masses [16][10]. If an even permutation (ijk) of the set (123) is considered, then the obtuse angle β_{ij} has the properties

$$\beta_{ij} = -\beta_{ji}, \quad \beta_{ii} = 0, \quad (4.13a)$$

$$\tan \beta_{ij} = -m_k/\mu, \quad (4.13b)$$

$$d_i d_j \sin \beta_{ij} = 1, \quad (4.13c)$$

$$d_i d_j m_k \cos \beta_{ij} = -\mu, \quad (4.13d)$$

$$\beta_{12} + \beta_{23} + \beta_{31} = 2\pi \quad (4.13e)$$

Orthogonal transformations within the coordinate set are then given by

$$\begin{pmatrix} \mathbf{r}_j \\ \mathbf{R}_j \end{pmatrix} = \begin{pmatrix} \cos \beta_{ij} & \sin \beta_{ij} \\ -\sin \beta_{ij} & \cos \beta_{ij} \end{pmatrix} \begin{pmatrix} \mathbf{r}_i \\ \mathbf{R}_i \end{pmatrix}. \quad (4.14)$$

4.2 The Hyperspherical Method

The next common step in the theoretical framework to describe systems of three particles is to introduce hyperspherical coordinates. The components of the two vectors \mathbf{r} and \mathbf{R} are combined into a single, six-dimensional position vector \mathbf{q} . The components of this vector can be regarded as the cartesian components of a point in \mathbb{R}^6 . The motion of the three particle system is thus equivalent to the motion of a single particle, with the reduced mass μ , in six-dimensional Euclidean space. The polar coordinates of this point particle are given by one hyperradial coordinate, ρ , and five hyperangular coordinates, collectively labelled Ω . Three of these hyperangles are the Euler angles associated with the orientation of the body fixed frame (i.e., the triangle formed by the three particles) in three-dimensional space, these are called external coordinates. The remaining two hyperangles describe the shape of the triangle, and the hyperradius describes the overall size of the system, these coordinates are the internal coordinates of the system. For the three-body problem, the hyperradius is defined by

$$\rho = \left(\mathbf{r}^2 + \mathbf{R}^2 \right)^{1/2}, \quad 0 \leq \rho < \infty. \quad (4.15)$$

Hyperspherical coordinates are useful for describing fragmentation problems. Fragmentations processes of the system into any one of the possible channels are described by the hyperradius becoming very large ($\rho \rightarrow \infty$), while the hyperangles distinguishes between the different fragmentation channels. The hyperradius invariant under both rotations and particle permutation. However, there are various ways to define the hyperangles and they are not in general invariant under particle permutations. The most common choices of parametrizing this hypersphere fall into two distinct categories: Delves coordinates, and (democratic) Smith-Whitten coordinates.

4.2.1 Delves Coordinates

Delves coordinates were originally developed to treat nuclear three-body problems. Numerical difficulties arise with Delves hyper angles when permutation symmetries for three identical particles is considered. Delves coordinates are adapted to collinear atom-diatom collisions and they are regular polar coordinates, where

$$r_k = \rho \sin \alpha_k \quad (4.16a)$$

$$R_k = \rho \cos \alpha_k. \quad (4.16b)$$

The Delves hyperangle α_k is then defined by

$$\alpha_k = \arctan \left(\frac{r_k}{R_k} \right), \quad 0 \leq \alpha_k \leq \frac{\pi}{2}. \quad (4.17)$$

This coordinate set corresponds to the reactant arrangement when particle k scatters of the weakly bound particles $i - j$. The other angle in this coordinate set is the angle between the two vectors \mathbf{r}_k and \mathbf{R}_k . It is given by

$$\cos \theta_k = \frac{\mathbf{r}_k \cdot \mathbf{R}_k}{r_k R_k}, \quad 0 \leq \theta \leq \pi. \quad (4.18)$$

Now, the massweighted Schrödinger equation for the stationary wavefunction Ψ of an n-body system with position vectors \mathbf{x}_i and masses m_i , ($i = 1, \dots, N$), interacting pairwise through a potential V , is given by

$$-\frac{\hbar^2}{2} \sum_{i=1}^N m_i^{-1} \nabla_{\mathbf{x}_i}^2 \Psi + V\Psi = E\Psi. \quad (4.19)$$

Where $\nabla^2 = \Delta$ is the Laplace operator, which in spherical coordinates reads

$$\Delta = \frac{1}{r^2} \frac{\partial}{\partial r} \left(r^2 \frac{\partial}{\partial r} \right) - \frac{\hat{L}^2}{\hbar^2 r^2}, \quad (4.20)$$

where \hat{L} is the angular momentum operator associated with the vector \mathbf{r} . And

$$\hat{L}^2 = -\hbar^2 \left(\frac{1}{\sin \theta} \frac{\partial}{\partial \theta} \left(\sin \theta \frac{\partial}{\partial \theta} \right) + \frac{1}{\sin^2 \theta} \frac{\partial^2}{\partial \phi^2} \right) \quad (4.21)$$

From now on $\hbar = 1$. The kinetic energy for three particles in the mass normalized Jacobi coordinates was given in (4.8). Next follows a derivation the kinetic energy operator in Delves hyperspherical coordinates. The Laplacians for the mass scaled Jacobi vectors are given by

$$\Delta_{r_k} = \frac{1}{r_k^2} \frac{\partial}{\partial r_k} \left(r_k^2 \frac{\partial}{\partial r_k} \right) - \frac{\hat{l}_{r_k}^2}{r_k^2} = \frac{2}{r_k} \frac{\partial}{\partial r_k} + \frac{\partial^2}{\partial r_k^2} - \frac{\hat{l}_{r_k}^2}{r_k^2} \quad (4.22a)$$

$$\Delta_{R_k} = \frac{1}{R_k^2} \frac{\partial}{\partial R_k} \left(R_k^2 \frac{\partial}{\partial R_k} \right) - \frac{\hat{l}_{R_k}^2}{R_k^2} = \frac{2}{R_k} \frac{\partial}{\partial R_k} + \frac{\partial^2}{\partial R_k^2} - \frac{\hat{l}_{R_k}^2}{R_k^2} \quad (4.22b)$$

If spin interactions are excluded the total orbital angular momentum is zero and we have

$$\hat{l}_{r_k}^2 = \hat{l}_{R_k}^2 = -\frac{1}{\sin \theta} \frac{\partial}{\partial \theta} \left(\sin \theta \frac{\partial}{\partial \theta} \right). \quad (4.23)$$

Change of coordinates into Delves polar coordinates results in the following transformations for the partial derivatives of the vector \mathbf{r}

$$\frac{\partial}{\partial r} = \frac{\partial \alpha}{\partial r} \frac{\partial}{\partial \alpha} + \frac{\partial \rho}{\partial r} \frac{\partial}{\partial \rho} = \frac{1}{\rho} \cos \alpha \frac{\partial}{\partial \alpha} + \sin \alpha \frac{\partial}{\partial \rho}, \quad (4.24a)$$

$$\begin{aligned} \frac{\partial^2}{\partial r^2} &= \left(\frac{1}{\rho} \cos \alpha \frac{\partial}{\partial \alpha} + \sin \alpha \frac{\partial}{\partial \rho} \right) \left(\frac{1}{\rho} \cos \alpha \frac{\partial}{\partial \alpha} + \sin \alpha \frac{\partial}{\partial \rho} \right) \\ &= \frac{1}{\rho^2} \cos^2 \alpha \frac{\partial^2}{\partial \alpha^2} - \frac{1}{\rho^2} \sin(2\alpha) \frac{\partial}{\partial \alpha} + \sin^2 \alpha \frac{\partial^2}{\partial \rho^2} \\ &\quad + \frac{1}{\rho} \cos^2 \alpha \frac{\partial}{\partial \rho} + \frac{1}{\rho} \sin(2\alpha) \frac{\partial^2}{\partial \alpha \partial \rho}. \end{aligned} \quad (4.24b)$$

Similarly, the partial derivatives with respect to the vector \mathbf{R} transform as

$$\frac{\partial}{\partial R} = \frac{\partial \alpha}{\partial R} \frac{\partial}{\partial \alpha} + \frac{\partial \rho}{\partial R} \frac{\partial}{\partial \rho} = -\frac{1}{\rho} \sin \alpha \frac{\partial}{\partial \alpha} + \cos \alpha \frac{\partial}{\partial \rho}, \quad (4.25a)$$

$$\begin{aligned} \frac{\partial^2}{\partial R^2} &= \left(-\frac{1}{\rho} \sin \alpha \frac{\partial}{\partial \alpha} + \cos \alpha \frac{\partial}{\partial \rho} \right) \left(-\sin \alpha \frac{\partial}{\partial \alpha} + \cos \alpha \frac{\partial}{\partial \rho} \right) \\ &= \frac{1}{\rho^2} \sin^2 \alpha \frac{\partial^2}{\partial \alpha^2} + \frac{1}{\rho^2} \sin(2\alpha) \frac{\partial}{\partial \alpha} + \cos^2 \alpha \frac{\partial^2}{\partial \rho^2} \\ &\quad + \frac{1}{\rho} \sin^2 \alpha \frac{\partial}{\partial \rho} - \frac{1}{\rho} \sin(2\alpha) \frac{\partial^2}{\partial \alpha \partial \rho}. \end{aligned} \quad (4.25b)$$

Finally, the sum of the two Laplacian operators now reads

$$\begin{aligned} \Delta_r + \Delta_R &= \frac{2}{r} \frac{\partial}{\partial r} + \frac{2}{R} \frac{\partial}{\partial R} + \frac{\partial^2}{\partial r^2} + \frac{\partial^2}{\partial R^2} - \frac{\hat{l}_r^2}{r^2} - \frac{\hat{l}_R^2}{R^2} \\ &= \frac{4}{\rho^2} \cot(2\alpha) \frac{\partial}{\partial \alpha} + \frac{5}{\rho} \frac{\partial}{\partial \rho} + \frac{1}{\rho^2} \frac{\partial^2}{\partial \alpha^2} + \frac{\partial^2}{\partial \rho^2} \\ &\quad + \frac{4}{\rho^2 \sin^2(2\alpha) \sin(\theta)} \frac{\partial}{\partial \theta} \left(\sin(\theta) \frac{\partial}{\partial \theta} \right) \\ &= \frac{1}{\rho^5} \frac{\partial}{\partial \rho} \left(\rho^5 \frac{\partial}{\partial \rho} \right) + \frac{1}{\rho^2 \sin^2(2\alpha)} \left(\frac{\partial}{\partial \alpha} \sin^2(2\alpha) \frac{\partial}{\partial \alpha} + \frac{4}{\sin \theta} \frac{\partial}{\partial \theta} \right). \end{aligned} \quad (4.26)$$

Thus in Delves hyperspherical coordinates the Schrödinger equation is given by

$$(\hat{T}_\rho + \hat{T}_{\alpha_k} + \hat{T}_\theta + V(\rho, \Omega)) \Psi = E \Psi, \quad (4.27)$$

where \hat{T}_ρ is the hyperradial kinetic energy operator,

$$\begin{aligned}
\hat{T}_\rho &= -\frac{\hbar^2}{2m} \left[\frac{1}{\rho^5} \frac{\partial}{\partial \rho} \left(\rho^5 \frac{\partial}{\partial \rho} \right) \right] \\
&= -\frac{\hbar^2}{2m} \left[\rho^{-5/2} \left(\rho^{5/2} \frac{5}{\rho} \frac{\partial}{\partial \rho} + \rho^{5/2} \frac{\partial^2}{\partial \rho^2} \right) \rho^{-5/2} \rho^{5/2} \right] \\
&= -\frac{\hbar^2}{2m} \rho^{-5/2} \left[-\frac{15}{4} \frac{1}{\rho^2} + \frac{\partial^2}{\partial \rho^2} \right] \rho^{5/2},
\end{aligned} \tag{4.28}$$

\hat{T}_α is the kinetic energy operator for the Delves angle α ,

$$\begin{aligned}
\hat{T}_\alpha &= -\frac{1}{2\mu} \frac{1}{\rho^2 \sin^2(2\alpha)} \left[\frac{\partial}{\partial \alpha} \sin^2(2\alpha) \frac{\partial}{\partial \alpha} \right] \\
&= -\frac{1}{2\mu} \frac{1}{\rho^2} \left[\frac{\partial^2}{\partial \alpha^2} + 4 \cot(2\alpha) \frac{\partial}{\partial \alpha} \right] \\
&= -\frac{1}{2\mu} \frac{1}{\rho^2} \left[\sin^{-1}(2\alpha) \left(\sin(2\alpha) \frac{\partial^2}{\partial \alpha^2} + 4 \cos(2\alpha) \frac{\partial}{\partial \alpha} \right) \sin^{-1}(2\alpha) \sin(2\alpha) \right] \\
&= -\frac{1}{2\mu} \frac{1}{\rho^2} \sin^{-1}(2\alpha) \left[\frac{\partial^2}{\partial \alpha^2} + 4 \right] \sin(2\alpha),
\end{aligned} \tag{4.29}$$

and \hat{T}_θ is the kinetic energy operator containing the angular momentum operators for the Jacobi vectors,

$$\begin{aligned}
\hat{T}_\theta &= -\frac{1}{2\mu} \left[\frac{4}{\rho^2 \sin^2(2\alpha) \sin(\theta)} \frac{\partial}{\partial \theta} \left(\sin(\theta) \frac{\partial}{\partial \theta} \right) \right] \\
&= -\frac{1}{2\mu} \left[\frac{1}{\rho^2 \sin^2 \alpha \cos^2 \alpha \sin \theta} \frac{\partial}{\partial \theta} \left(\sin \theta \frac{\partial}{\partial \theta} \right) \right]
\end{aligned} \tag{4.30}$$

The Hamiltonian operator is given by

$$H_0 = \hat{T}_\rho + \hat{T}_\alpha + \hat{T}_\theta + V(\rho, \Omega). \tag{4.31}$$

Removal of first derivatives with respect to ρ and α is possible by writing the wavefunction as $\Psi = \rho^{-5/2} (\sin(2\alpha))^{-1} \psi$. The corresponding transformation of the Hamiltonian is then

$$\begin{aligned}
H - V &= \rho^{5/2} \sin(2\alpha) (H_0 - V) \rho^{-5/2} (\sin(2\alpha))^{-1} \\
&= -\frac{1}{2\mu} \left[\frac{\partial^2}{\partial \rho^2} - \frac{15}{4\rho^2} + \frac{1}{\rho^2} \left(\frac{\partial^2}{\partial \alpha^2} + 4 + \frac{1}{\sin^2 \alpha \cos^2 \alpha \sin \theta} \frac{\partial}{\partial \theta} \left(\sin \theta \frac{\partial}{\partial \theta} \right) \right) \right] \\
&= -\frac{1}{2\mu} \left[\frac{\partial^2}{\partial \rho^2} + \frac{1}{\rho^2} \left(\frac{\partial^2}{\partial \alpha^2} + \frac{1}{\sin^2 \alpha \cos^2 \alpha \sin \theta} \frac{\partial}{\partial \theta} \left(\sin \theta \frac{\partial}{\partial \theta} \right) \right) + \frac{1}{4\rho^2} \right] \\
&= -\frac{1}{2\mu} \frac{\partial^2}{\partial \rho^2} + \frac{\Lambda^2 - 1/4}{2\mu \rho^2},
\end{aligned} \tag{4.32}$$

where Λ^2 is the hyperangular kinetic energy, also called the grand angular momentum operator since it is the angular momentum in this six dimensional space, it is in this case given by

$$\Lambda^2 = -\frac{\partial^2}{\partial \alpha^2} - \frac{1}{\sin^2 \alpha \cos^2 \alpha \sin \theta} \frac{\partial}{\partial \theta} \left(\sin \theta \frac{\partial}{\partial \theta} \right). \quad (4.33)$$

The volume element is proportional to $\rho^5 \sin^2 \alpha \cos^2 \alpha \sin \theta d\rho d\alpha d\theta$. The wavefunction needs to be square-integrable, so $\Psi = 0$ at $\rho = 0$ and $\alpha = 0$ or π . Further,

$$\begin{aligned} \psi(0, \alpha, \theta) &= 0 \\ \psi(\rho, 0, \theta) &= \psi(\rho, \frac{\pi}{2}, \theta) = 0 \\ \frac{\partial \psi}{\partial \theta} \Big|_{\theta=0} &= \frac{\partial \psi}{\partial \theta} \Big|_{\theta=\pi} = 0 \end{aligned}$$

4.2.2 Smith-Whitten Coordinates

In this section, we show how the three-body system can be represented in a symmetric way. The derivation of the Hamiltonian for this representation is described using a modified set of Smith-Whitten – or democratic – coordinates.

At any instant, three particles form a plane in \mathbb{R}^3 . If we consider this plane to be the x-y plane, and define the internal motion of the particles within this plane in terms of hyperspherical coordinates, our coordinate system must rotate in this plane. That is, we use a body-fixed coordinate system XYZ , which rotates with respect to the space fixed axis $X'Y'Z'$. [Details](spatial rotation). The internal coordinates ρ , Θ , and Φ determine the size and shape of the triangle formed by the three particle system. With the z -axis perpendicular to the plane, Smith and Whitten [ref] defined these as

$$\begin{aligned} r_x &= \rho \cos(\Theta) \cos(\Phi), \\ r_y &= -\rho \sin(\Theta) \sin(\Phi), \\ r_z &= 0 \\ R_x &= \rho \cos(\Theta) \sin(\Phi), \\ R_y &= \rho \sin(\Theta) \cos(\Phi), \\ R_z &= 0. \end{aligned}$$

The distance between the particles are given by

$$x_3 = d_3 \mid \mathbf{r}_3 \mid = \frac{\rho d_3}{2^{1/2}} [1 + \cos(2\Theta) \cos(2\Phi_3)]^{1/2} \quad (4.36)$$

$$x_1 = d_1 \mid \mathbf{r}_1 \mid = d_1 [\cos^2 \beta_{31} \mathbf{r}_3^2 + \sin^2 \beta_{31} \mathbf{R}_3^2 + 2 \sin \beta_{31} \cos \beta_{31} \mathbf{r}_3 \cdot \mathbf{R}_3]^{1/2} \quad (4.37)$$

$$\begin{aligned} &= \frac{d_1 \rho}{2^{1/2}} [\cos^2 \beta_{31} (1 + \cos(2\Theta) \cos(2\Phi_3)) \\ &\quad + \sin^2 \beta_{31} (1 - \cos(2\Theta) \cos(2\Phi_3)) \\ &\quad + 2 \sin \beta_{31} \cos \beta_{31} \cos(2\Theta) \sin(2\Phi_3)]^{1/2} \\ &= \frac{d_1 \rho}{2^{1/2}} [1 + \cos(2\Theta) (\cos(\Phi_3) \cos(2\beta_{31}) + \sin(2\Phi_3) \sin(2\beta_{31}))]^{1/2} \\ &= \frac{d_1 \rho}{2^{1/2}} [1 + \cos(2\Theta) \cos(2\Phi_3 - 2\beta_{31})]^{1/2} \\ &= \frac{d_1 \rho}{2^{1/2}} [1 + \cos(2\Theta) \cos(2\Phi_1)]^{1/2} \\ x_2 &= d_2 \mid \mathbf{r}_2 \mid = d_2 [\cos^2 \beta_{23} \mathbf{r}_3^2 + \sin^2 \beta_{23} \mathbf{R}_3^2 - 2 \sin \beta_{23} \cos \beta_{23} \mathbf{r}_3 \cdot \mathbf{R}_3]^{1/2} \\ &= \frac{d_2 \rho}{2^{1/2}} [1 + \cos(2\Theta) (\cos(\Phi_3) \cos(2\beta_{23}) - \sin(2\Phi_3) \sin(2\beta_{23}))]^{1/2} \\ &= \frac{d_1 \rho}{2^{1/2}} [1 + \cos(2\Theta) \cos(2\Phi_3 + 2\beta_{23})]^{1/2} \\ &= \frac{d_1 \rho}{2^{1/2}} [1 + \cos(2\Theta) \cos(2\Phi_2)]^{1/2} \end{aligned}$$

Thus, $\Phi_j = \Phi_i - \beta_{ij}$ and

$$x_k = \frac{d_k \rho}{2^{1/2}} [1 + \cos(2\Theta) \cos(2\Phi_k)]^{1/2}. \quad (4.38)$$

Now we choose $\Phi_3 = \Phi$

$$x_3 = \frac{\rho d_3}{2^{1/2}} [1 + \cos(2\Theta) \cos(2\Phi)]^{1/2} \quad (4.39)$$

$$x_1 = \frac{d_1 \rho}{2^{1/2}} [1 + \cos(2\Theta) \cos(2\Phi + \epsilon_1)]^{1/2} \quad (4.40)$$

$$x_2 = \frac{d_1 \rho}{2^{1/2}} [1 + \cos(2\Theta) \cos(2\Phi + \epsilon_2)]^{1/2} \quad (4.41)$$

where

$$\epsilon_1 = -2 \tan^{-1}(-m_2/\mu) \quad (4.42)$$

$$\epsilon_2 = 2 \tan^{-1}(-m_1/\mu) \quad (4.43)$$

Now for three identical particles we get

$$x_3 = \frac{\rho}{3^{1/4}} [1 + \cos(2\Theta) \cos(2\Phi)]^{1/2} \quad (4.44)$$

$$x_1 = \frac{\rho}{3^{1/4}} [1 + \cos(2\Theta) \cos(2\Phi - 4\pi/3)]^{1/2} \quad (4.45)$$

$$x_2 = \frac{\rho}{3^{1/4}} [1 + \cos(2\Theta) \cos(2\Phi + 4\pi/3)]^{1/2} \quad (4.46)$$

Now, with $\phi_k = \pi/2 - 2\Phi_k$, we get $\phi_j = \phi_i + 2\beta_{ij}$, where $(-7\pi/2 \leq \phi_k < \pi/2)$. Now with $2\beta_{ij} = -2\eta_{ij}$ and

$$\eta_{ij} = -\eta_{ji}, \quad \eta_{ii} = 0, \quad (4.47)$$

$$\tan \eta_{ij} = m_k/\mu, \quad (4.48)$$

$$\eta_{12} + \eta_{23} + \eta_{31} = \pi \quad (4.49)$$

We get

$$x_k = \frac{d_k \rho}{2^{1/2}} [1 + \sin \theta \sin \phi_k]^{1/2}. \quad (4.50)$$

$$x_3 = \frac{d_3 \rho}{2^{1/2}} [1 + \sin \theta \sin \phi]^{1/2} \quad (4.51)$$

$$x_1 = \frac{d_1 \rho}{2^{1/2}} [1 + \sin \theta \sin(\phi - \varphi_1)]^{1/2} \quad (4.52)$$

$$x_2 = \frac{d_1 \rho}{2^{1/2}} [1 + \sin \theta \sin(\phi + \varphi_2)]^{1/2} \quad (4.53)$$

$$\varphi_1 = 2 \tan^{-1}(m_2/\mu) \quad (4.54)$$

$$\varphi_2 = 2 \tan^{-1}(m_1/\mu) \quad (4.55)$$

Now we redefine $\phi'_k = \phi_k + 7\pi/2$, so that the range is $0 \leq \phi'_k < 4\pi$. Then $\sin \phi_k = \cos \phi'_k$. We finally get ($2\Phi = 4\pi - \phi'$)

$$x_3 = \frac{d_3 \rho}{2^{1/2}} [1 + \sin \theta \cos \phi']^{1/2} \quad (4.56)$$

$$x_1 = \frac{d_1 \rho}{2^{1/2}} [1 + \sin \theta \cos(\phi' - \varphi_1)]^{1/2} \quad (4.57)$$

$$x_2 = \frac{d_1 \rho}{2^{1/2}} [1 + \sin \theta \cos(\phi' + \varphi_2)]^{1/2}. \quad (4.58)$$

This is the same expression as Blume and Wang get, however the define there angles slightly different. Our interval is two times Blumes interval

The area of the triangle formed by the three particles is the length of the vector given by

$$\mathbf{A} = \frac{1}{2}(\mathbf{r} \times \mathbf{R}) \quad (4.59)$$

$$A = \frac{1}{2}(r_x R_y - r_y R_x) = \frac{1}{4}\rho^2 \sin(2\Theta) \quad (4.60)$$

$$\sin 2\Theta = 4A/\rho^2 \quad (4.61)$$

Since both the area and the hyperradius are positive quantities the angle must be in the range, $0 \leq \Theta \leq \pi/4$. For some reason $0 \leq \Phi < 2\pi$. The transformed coordinates then have the range $0 \leq \theta \leq \pi/2$ and

To describe how rotations of the BF system affects the derivatives in the SF system, introduce the infinitesimal rotations ω . The velocities of the SF system vectors are given by

$$\begin{aligned} \dot{\mathbf{r}}' &= \dot{\mathbf{r}} + \omega \times \mathbf{r} \\ \dot{\mathbf{R}}' &= \dot{\mathbf{R}} + \omega \times \mathbf{R} \end{aligned}$$

which is given explicitly by

$$\begin{aligned} \begin{pmatrix} \dot{r}'_x \\ \dot{r}'_y \\ \dot{r}'_z \\ \dot{R}'_x \\ \dot{R}'_y \\ \dot{R}'_z \end{pmatrix} &= \begin{pmatrix} \partial_\rho r_x & \partial_\Theta r_x & \partial_\Theta r_x & 0 & r_z & -r_y \\ \partial_\rho r_y & \partial_\Theta r_y & \partial_\Theta r_y & -r_z & 0 & r_x \\ \partial_\rho r_z & \partial_\Theta r_z & \partial_\Theta r_z & r_y & -r_x & 0 \\ \partial_\rho R_x & \partial_\Theta R_x & \partial_\Theta R_x & 0 & R_z & -R_y \\ \partial_\rho R_y & \partial_\Theta R_y & \partial_\Theta R_y & -R_z & 0 & R_x \\ \partial_\rho R_z & \partial_\Theta R_z & \partial_\Theta R_z & R_y & -R_x & 0 \end{pmatrix} \begin{pmatrix} \dot{\rho} \\ \dot{\Theta} \\ \dot{\Phi} \\ \omega_x \\ \omega_y \\ \omega_z \end{pmatrix} \\ &= \begin{pmatrix} cc & -sc & -cs & 0 & 0 & ss \\ -ss & -cs & -sc & 0 & 0 & cc \\ 0 & 0 & 0 & -ss & -cc & 0 \\ cs & -ss & cc & 0 & 0 & -sc \\ sc & cc & -ss & 0 & 0 & cs \\ 0 & 0 & 0 & sc & -cs & 0 \end{pmatrix} \begin{pmatrix} \dot{\rho} \\ \rho\dot{\Theta} \\ \rho\dot{\Phi} \\ \rho\omega_x \\ \rho\omega_y \\ \rho\omega_z \end{pmatrix} \end{aligned} \quad (4.63)$$

$$(4.64)$$

In matrix notation:

$$\dot{\mathbf{q}}' = \hat{A}\dot{\mathbf{q}}, \quad (4.65)$$

where

$$\dot{\mathbf{q}}' = \begin{pmatrix} \dot{r}'_x \\ \dot{r}'_y \\ \dot{r}'_z \\ \dot{R}'_x \\ \dot{R}'_y \\ \dot{R}'_z \end{pmatrix}, \dot{\mathbf{q}} = \begin{pmatrix} \dot{\rho} \\ \dot{\Theta} \\ \dot{\Phi} \\ \omega_x \\ \omega_y \\ \omega_z \end{pmatrix}$$

The arclength is given by

$$s = \int_a^b \|\dot{\mathbf{q}}'\| dt = \int_a^b \sqrt{\dot{\mathbf{q}}'^T \dot{\mathbf{q}}'} dt \quad (4.66)$$

and

$$(ds)^2 = (d\mathbf{q}')^T (d\mathbf{q}') = d\mathbf{q}^T \hat{A}^T \hat{A} d\mathbf{q} = d\mathbf{q}^T \mathbf{g} d\mathbf{q}, \quad (4.67)$$

where \mathbf{g} is the metric tensor

$$\mathbf{g} = \begin{pmatrix} \mathbf{G} & \mathbf{C} \\ \mathbf{C}^T & \mathbf{K} \end{pmatrix} \quad (4.68)$$

where the submatrices \mathbf{G} , \mathbf{K} and \mathbf{C} are

$$\mathbf{G} = \begin{pmatrix} 1 & 0 & 0 \\ 0 & \rho^2 & 0 \\ 0 & 0 & \rho^2 \end{pmatrix} \quad (4.69)$$

$$\mathbf{K} = \rho^2 \begin{pmatrix} \sin^2 \Theta & 0 & 0 \\ 0 & \cos^2 \Theta & 0 \\ 0 & 0 & 1 \end{pmatrix} \quad (4.70)$$

$$\mathbf{C} = -\rho^2 \sin^2(2\Theta) \begin{pmatrix} 0 & 0 & 0 \\ 0 & 0 & 0 \\ 0 & 0 & 1 \end{pmatrix} \quad (4.71)$$

the inverse of the metric tensor \mathbf{g}^{-1}

$$\mathbf{g}^{-1} = \begin{pmatrix} \mathbf{V} & \mathbf{W} \\ \mathbf{W}^T & \mathbf{U} \end{pmatrix} \quad (4.72)$$

where the submatrices \mathbf{V} , \mathbf{W} and \mathbf{U} are

$$\mathbf{V} = \begin{pmatrix} 1 & 0 & 0 \\ 0 & 1/\rho^2 & 0 \\ 0 & 0 & 1/\rho^2 \cos^2(2\Theta) \end{pmatrix} \quad (4.73)$$

$$\mathbf{U} = \frac{1}{\rho^2} \begin{pmatrix} 1/\sin^2 \Theta & 0 & 0 \\ 0 & 1/\cos^2 \Theta & 0 \\ 0 & 0 & 1/\cos^2(2\Theta) \end{pmatrix} \quad (4.74)$$

$$\mathbf{W} = \frac{\sin(2\Theta)}{\rho^2 \cos^2(2\Theta)} \begin{pmatrix} 0 & 0 & 0 \\ 0 & 0 & 0 \\ 0 & 0 & 1 \end{pmatrix} \quad (4.75)$$

The determinant of the metric tensor is given by

$$g = |\mathbf{g}| = \begin{vmatrix} \mathbf{G} & \mathbf{C} \\ \mathbf{C}^T & \mathbf{K} \end{vmatrix} = \begin{vmatrix} \mathbf{G} & \mathbf{C} \\ 0 & \mathbf{K} - \mathbf{C}^T \mathbf{G}^{-1} \mathbf{C} \end{vmatrix} \quad (4.76)$$

$$= |\mathbf{G}| \cdot |\mathbf{K} - \mathbf{C}^T \mathbf{G}^{-1} \mathbf{C}| = \frac{\rho^{10}}{16} \sin^2(4\Theta) \quad (4.77)$$

$$\sqrt{g} = \frac{\rho^5}{4} \sin(4\Theta) \quad (4.78)$$

The kinetic energy operator of a particle with mass μ in a curvilinear coordinate system of N dimensions is given by

$$T = -\frac{\hbar^2}{2\mu} \sum_{i=1}^N \sum_{j=1}^N \frac{1}{\sqrt{g}} \frac{\partial}{\partial q_i} \left(\sqrt{g} g^{ij} \frac{\partial}{\partial q_j} \right) \quad (4.79)$$

where g^{ij} is the inverse metric tensor. The momentum vector is given by

$$\mathbf{p} = i\hbar \begin{pmatrix} \partial/\partial q_1 \\ \vdots \\ \partial/\partial q_N \end{pmatrix} \quad (4.80)$$

With ω expressed in Euler angles

$$\omega = \begin{pmatrix} d\Omega_x \\ d\Omega_y \\ d\Omega_z \end{pmatrix} \quad (4.81)$$

we get the kinetic energy

$$\begin{aligned}
-\frac{1}{\hbar^2}\hat{T} &= -\frac{1}{2\mu\rho^5\sin(4\Theta)}\mathbf{p}^T\left(\rho^5\sin(4\Theta)\mathbf{g}^{-1}\right)\mathbf{p} \\
&= \frac{1}{2\mu\rho^5\sin(4\Theta)}\left[\frac{\partial}{\partial\rho}\left(\rho^5\sin(4\Theta)\frac{\partial}{\partial\rho}\right) + \frac{\partial}{\partial\Theta}\left(\rho^3\sin(4\Theta)\frac{\partial}{\partial\Theta}\right) \right. \\
&\quad + \frac{\partial}{\partial\Phi}\left(2\rho^3\tan(2\Theta)\frac{\partial}{\partial\Phi} + 2\tan^2(2\Theta)\cos(2\Theta)\frac{\partial}{\partial\Omega_z}\right) \\
&\quad + \frac{\partial}{\partial\Omega_x}\left(4\rho^3\cot(\Theta)\cos(2\Theta)\frac{\partial}{\partial\Omega_x}\right) \\
&\quad + \frac{\partial}{\partial\Omega_y}\left(4\rho^3\tan(2\Theta)\cos(2\Theta)\frac{\partial}{\partial\Omega_y}\right) \\
&\quad \left. + \frac{\partial}{\partial\Omega_z}\left(2\rho^3\tan^2(2\Theta)\frac{\partial}{\partial\Phi} + 2\rho^3\tan(2\Theta)\frac{\partial}{\partial\Omega_z}\right)\right] \\
&= \frac{1}{2\mu}\left[\frac{1}{\rho^5}\frac{\partial}{\partial\rho}\left(\rho^5\frac{\partial}{\partial\rho}\right) + \frac{1}{\rho^2\sin(4\Theta)}\frac{\partial}{\partial\Theta}\left(\sin(4\Theta)\frac{\partial}{\partial\Theta}\right) \right. \\
&\quad + \frac{1}{\rho^2\cos^2(2\Theta)}\frac{\partial^2}{\partial\Phi^2} + \frac{\sin(2\Theta)}{\rho^2\cos^2(2\Theta)}\frac{\partial}{\partial\Phi}\frac{\partial}{\partial\Omega_z} \\
&\quad + \frac{1}{\rho^2\sin^2(\Theta)}\frac{\partial^2}{\partial\Omega_x^2} + \frac{1}{\rho^2\cos^2(\Theta)}\frac{\partial^2}{\partial\Omega_y^2} + \frac{\sin(2\Theta)}{\rho^2\cos^2(2\Theta)}\frac{\partial}{\partial\Omega_z}\frac{\partial}{\partial\Phi} \\
&\quad \left. + \frac{1}{\rho^2\cos^2(2\Theta)}\frac{\partial^2}{\partial\Omega_z^2}\right] \\
&= \frac{1}{2\mu\rho^5}\frac{\partial}{\partial\rho}\left(\rho^5\frac{\partial}{\partial\rho}\right) + \frac{1}{2\mu\rho^2}\left[\frac{1}{\sin(4\Theta)}\frac{\partial}{\partial\Theta}\left(\sin(4\Theta)\frac{\partial}{\partial\Theta}\right) \right. \\
&\quad + \frac{1}{\cos^2(2\Theta)}\frac{\partial^2}{\partial\Phi^2}\left] + \frac{1}{2\mu\rho^2}\left[\frac{1}{\sin^2(\Theta)}\frac{\partial^2}{\partial\Omega_x^2} + \frac{1}{\cos^2(\Theta)}\frac{\partial^2}{\partial\Omega_y^2} + \frac{1}{\cos^2(2\Theta)}\frac{\partial^2}{\partial\Omega_z^2} \right. \\
&\quad \left. + \frac{2\sin(2\Theta)}{\cos^2(2\Theta)}\frac{\partial}{\partial\Phi}\frac{\partial}{\partial\Omega_z}\right].
\end{aligned}$$

The volume element in a general coordinate system of N dimensions is given by

$$d^N v = g^{1/2} \prod_{i=1}^N dq_i \quad (4.82)$$

The Euler angles are given by

$$\begin{pmatrix} d\Omega_x \\ d\Omega_y \\ d\Omega_z \end{pmatrix} = \mathbf{A} \begin{pmatrix} d\alpha \\ d\beta \\ d\gamma \end{pmatrix} \quad (4.83)$$

where

$$\mathbf{A} = \begin{pmatrix} -\sin\beta \cos\gamma & \sin\gamma & 0 \\ \sin\beta \sin\gamma & \cos\gamma & 0 \\ \cos\beta & 0 & 1 \end{pmatrix} \quad (4.84)$$

$$d\mathbf{q} = \begin{pmatrix} d\rho \\ d\Theta \\ d\Phi \\ d\Omega_x \\ d\Omega_y \\ d\Omega_z \end{pmatrix}, d\mathbf{q}' = \begin{pmatrix} d\rho \\ d\Theta \\ d\Phi \\ d\alpha \\ d\beta \\ d\gamma \end{pmatrix}$$

$$ds^2 = (d\mathbf{q})^T \mathbf{g} d\mathbf{q} = (d\mathbf{q}')^T \mathbf{g}' d\mathbf{q}' \quad (4.85)$$

with

$$\mathbf{B} = \begin{pmatrix} \mathbf{I} & 0 \\ 0 & \mathbf{A} \end{pmatrix} \quad (4.86)$$

$$\mathbf{g}' = \mathbf{B}^T \mathbf{g} \mathbf{B} \quad (4.87)$$

and the determinant is then

$$g'^{1/2} = (|\mathbf{B}|^2 |\mathbf{g}|)^{1/2} = (|\mathbf{A}|^2 |\mathbf{g}|)^{1/2} = \frac{\rho^5}{4} \sin(4\Theta) \sin\beta \quad (4.88)$$

In our set up we thus get

$$d^6v = g^{1/2} \prod_{i=1}^6 dq_i = \frac{\rho^5}{4} \sin(4\Theta) \sin\beta d\rho d\Theta d\Phi d\alpha d\beta d\gamma \quad (4.89)$$

Now, we make a transformation of the angles (Kupfermann)

$$\Theta = \pi/4 - \theta/2$$

$$\Phi = \pi/4 - \phi/2$$

and

$$\frac{\partial}{\partial\Theta} = -2 \frac{\partial}{\partial\theta}$$

$$\frac{\partial}{\partial\Phi} = -2 \frac{\partial}{\partial\phi}$$

$$\begin{aligned}
\sin(4\Theta) &= \sin(2\theta) \\
\cos^2(2\Theta) &= \sin^2(\theta) \\
\sin^2(2\Theta) &= \cos^2(\theta) \\
\cos^2 \Theta &= \frac{1}{2}(1 + \sin \theta) \\
\sin^2 \Theta &= \frac{1}{2}(1 - \sin \theta)
\end{aligned}$$

The corresponding volume element is then

$$d^6v = \frac{1}{8} \rho^5 \sin \theta \cos \theta \sin \beta d\rho d\theta d\phi d\alpha d\beta d\gamma \quad (4.90)$$

Now with

$$\mathbf{P} = -i\hbar \begin{pmatrix} \partial/\partial\rho \\ \partial/\partial\theta \\ \partial/\partial\phi \end{pmatrix} = \begin{pmatrix} P_\rho \\ P_\theta \\ P_\phi \end{pmatrix} \quad (4.91)$$

and

$$\mathbf{J} = -i\hbar \begin{pmatrix} \partial/\partial\Omega_x \\ \partial/\partial\Omega_y \\ \partial/\partial\Omega_z \end{pmatrix} = \begin{pmatrix} J_x \\ J_y \\ J_z \end{pmatrix} \quad (4.92)$$

The kinetic energy operator then becomes

$$\begin{aligned}
\hat{T} = & -\frac{\hbar^2}{2\mu} \left[\frac{1}{\rho^5} \frac{\partial}{\partial\rho} \rho^5 \frac{\partial}{\partial\rho} + \frac{4}{\rho^2} \left(\frac{1}{\sin(2\theta)} \frac{\partial}{\partial\theta} \sin(2\theta) \frac{\partial}{\partial\theta} \right. \right. \\
& \left. \left. + \frac{1}{\sin^2(\theta)} \frac{\partial^2}{\partial\phi^2} \right) \right] - \frac{1}{\mu\rho^2} \left[\frac{J_x^2}{(1 - \sin \theta)} + \frac{J_y^2}{(1 + \sin \theta)} + \frac{J_z^2}{2 \sin^2 \theta} \right] \\
& + \frac{4i\hbar \cos \theta J_z}{2\mu\rho^2 \sin^2 \theta} \frac{\partial}{\partial\phi}
\end{aligned}$$

If we only consider $J = 0$ states, the Hamiltonian reduces to

$$H_0 = -\frac{\hbar^2}{2\mu} \left[\frac{1}{\rho^5} \frac{\partial}{\partial\rho} \rho^5 \frac{\partial}{\partial\rho} + \frac{4}{\rho^2} \left(\frac{1}{\sin(2\theta)} \frac{\partial}{\partial\theta} \sin(2\theta) \frac{\partial}{\partial\theta} + \frac{1}{\sin^2(\theta)} \frac{\partial^2}{\partial\phi^2} \right) \right] + V(\rho, \theta, \phi) \quad (4.93)$$

By making the following transformation of the wave function

$$\psi = \rho^{5/2} \Psi, \quad (4.94)$$

the Schrödinger equation becomes

$$H\psi = E\psi. \quad (4.95)$$

Where the transformed Hamiltonian operator is given by

$$H = \rho^{5/2} H_0 \rho^{-5/2}. \quad (4.96)$$

This transformation removes the first derivative in the hyper radial kinetic-energy operator since

$$T_\rho = \rho^{5/2} T_{\rho_0} \rho^{-5/2} = \rho^{5/2} \frac{1}{\rho^5} \frac{\partial}{\partial \rho} \rho^5 \frac{\partial}{\partial \rho} (\rho^{-5/2}) = -\frac{15}{4} \frac{1}{\rho^2} + \frac{\partial^2}{\partial \rho^2} \quad (4.97)$$

and we get the final expression for the Hamiltonian

$$H = -\frac{\hbar^2}{2\mu} \left[-\frac{15}{4} \frac{1}{\rho^2} + \frac{\partial^2}{\partial \rho^2} + \frac{4}{\rho^2} \left(\frac{1}{\sin(2\theta)} \frac{\partial}{\partial \theta} \sin(2\theta) \frac{\partial}{\partial \theta} + \frac{1}{\sin^2(\theta)} \frac{\partial^2}{\partial \phi^2} \right) \right] + V(\rho, \theta, \phi) \quad (4.98)$$

$$= -\frac{\hbar^2}{2\mu\rho^2} \frac{\partial^2}{\partial \rho^2} + \frac{\hbar^2}{2\mu\rho^2} \left(\Lambda^2 + \frac{15}{4} \right) + V(\rho, \theta, \phi), \quad (4.99)$$

where Λ^2 is the grand angular momentum operator.

4.2.3 Symmetries

The Smith-Whitten coordinates θ and ϕ are connected to the geometry of the triangle formed by the three particles. If the three particles represent the vertex of a triangle, θ will determine its shape, while ϕ determines the arrangement of the particles at its vertex. Now let's determine the eigenvalues and eigenfunctions of the grand angular momentum operator. For the ϕ equation we have

$$\frac{\partial^2}{\partial \phi^2} e^{i\nu\phi} = -\nu^2 e^{i\nu\phi}, \quad (4.100)$$

so the total eigenfunction can be written

$$f_{\nu n}(\theta, \phi) = g_{\nu n}(\theta) e^{i\nu\phi}. \quad (4.101)$$

For a general system we have the symmetry

$$f_{\nu n}(\theta, \phi = 0) = \Pi f_{\nu n}(\theta, \phi = 2\pi), \quad \text{for} \quad \Pi = \pm 1, \quad (4.102)$$

the symmetry of a three identical particle system will reduce the interval of ϕ to $[0, 2\pi/3]$. (symmetry group C_{3v} with irreducible representations A_1 , A_2 , and E), we will consider bosons and states with $J = 0$ so this leads to vibrational

wave functions of A_1 symmetry and this will reduce the interval of ϕ further to $[0, \pi/3]$, so

$$f_{\nu n}(\theta, \phi = 0) = \Pi f_{\nu n}(\theta, \phi = 2\pi/3), \quad \text{for} \quad \Pi = \pm 1, \quad (4.103)$$

where the parity $\Pi = 1$ for bosons. Thus

$$e^{i\nu 2\pi/3} = 1 \quad \Leftrightarrow \quad \nu = 3n \quad \text{for} \quad n = 0, 1, 2, \dots \quad (4.104)$$

so we get

$$\Lambda^2 g_{\nu\nu}(\theta) = -4 \left(\frac{1}{\sin(2\theta)} \frac{\partial}{\partial \theta} \sin(2\theta) \frac{\partial}{\partial \theta} - \frac{\nu^2}{\sin^2(\theta)} \right) g_{\nu\nu}(\theta) = \lambda_{\nu\nu} g_{\nu\nu}(\theta). \quad (4.105)$$

The interval for θ is $[0, \pi/2]$. Lets look at the boundary as $\theta \rightarrow 0$. The small angle approximation leads to

$$\Lambda^2 \rightarrow -4 \left(\frac{1}{\theta} \frac{\partial}{\partial \theta} + \frac{\partial^2}{\partial \theta^2} - \frac{\nu^2}{\theta^2} \right) g_{\nu\nu}(\theta) = \lambda_{\nu\nu} g_{\nu\nu}(\theta). \quad (4.106)$$

we thus need to solve a differential equation of the form

$$g_{\nu\nu}''(\theta) + \frac{P(\theta)}{\theta} g_{\nu\nu}'(\theta) + \frac{Q(\theta)}{\theta^2} g_{\nu\nu}(\theta) = 0, \quad (4.107)$$

with

$$P(\theta) = 1 \quad \text{and} \quad Q(\theta) = \frac{\lambda_{\nu\nu}\theta^2 - 4\nu^2}{4}. \quad (4.108)$$

Since ref[the differential equation] has a regular singular point at $\theta = 0$ and both $P(\theta)$ and $Q(\theta)$ are analytic functions, we seek a power series solution of the form

$$g_{\nu\nu}(\theta) = \sum_{k=0}^{\infty} A_k \theta^{k+s}, \quad (A_0 \neq 0). \quad (4.109)$$

differentiating

$$g_{\nu\nu}'(\theta) = \sum_{k=0}^{\infty} (k+s) A_k \theta^{k+s-1}, \quad (4.110)$$

$$g_{\nu\nu}''(\theta) = \sum_{k=0}^{\infty} (k+s)(k+s-1) A_k \theta^{k+s-2}, \quad (4.111)$$

and substituting into [ref] we get

$$\sum_{k=0}^{\infty} \left((k+s)(k+s-1) + (k+s) - \nu^2 \right) A_k \theta^{k+s-2} + \left(\frac{\lambda_{n\nu}}{4} \right) A_k \theta^{k+s} =$$

$$[s(s-1) + s - \nu^2] A_0 \theta^{s-2} + \sum_{k=1}^{\infty} \left([(k+s)(k+s-1) + (k+s) - \nu^2] A_k + \frac{\lambda_{n\nu}}{4} A_{k-2} \right) \theta^{k+s-2}$$

From $s^2 - \nu^2 = 0$ we get the two roots $s = \pm\nu$. Using these roots, we set the coefficients of θ^{k+s-2} to be zero, and we get the equations

$$(k^2 \pm 2k\nu) A_k = \frac{\lambda_{n\nu}}{4} A_{k-2} \quad (4.112)$$

The table 1 shows the analytically derived eigenvalues in SW-coordinates.

$\nu = 0$	$\nu = 3$	$\nu = 6$	Total	$\lambda(\lambda + 4)$	multiplicity
0	60	192	0	0	1
32	140	320	32	4	1
96	252	480	60	6	1
192	396	672	96	8	1
320	572	896	140	10	1
480	780	1152	192	12	2
672	1020	1440	252	14	1

Table 1: Analytically derived eigenvalues

4.3 Adiabatic hyperspherical method

In the following sections we have chosen to work in the set of democratic hyperangles described in 4.2.2. With these coordinates, the Schrödinger equation for the internal coordinates was derived as

$$\left(-\frac{1}{2\mu} \frac{\partial^2}{\partial \rho^2} + \frac{\Lambda^2 + 15/4}{2\mu\rho^2} + V(\rho, \theta, \phi) \right) \psi(\rho, \theta, \phi) = E\psi(\rho, \theta, \phi), \quad (4.113)$$

with boundary conditions

$$\frac{\partial \Phi_\nu(\rho; 0, \phi)}{\partial \theta} = \frac{\partial \Phi_\nu(\rho; \frac{\pi}{2}, \phi)}{\partial \theta}, \quad (4.114)$$

$$\frac{\partial \Phi_\nu(\rho; \theta, 0)}{\partial \phi} = \frac{\partial \Phi_\nu(\rho; \theta, \frac{2\pi}{3})}{\partial \phi}, \quad (4.115)$$

reflecting three identical particle symmetry. We assume that the interactions V can be written as a sum of pairwise two-body potentials

$$V(\rho, \theta, \psi) = v(r_k) + v(r_i) + v(r_j). \quad (4.116)$$

The two-body interaction

$$v(r) = d \cosh^{-2}(r/r_0). \quad (4.117)$$

$$r_3 = 3^{-1/4} \rho [1 + \sin \theta \cos \phi]^{1/2} \quad (4.118)$$

$$r_1 = 3^{-1/4} \rho [1 + \sin \theta \cos(\phi - 2\pi/3)]^{1/2} \quad (4.119)$$

$$r_2 = 3^{-1/4} \rho [1 + \sin \theta \cos(\phi + 2\pi/3)]^{1/2} \quad (4.120)$$

The exact solution to (4.113) can be found by first writing $\psi_n(\rho, \theta, \phi)$ as an expansion of radial wavefunctions $F_{n\nu}(\rho)$ and a set of complete, orthonormal channel functions $\Phi_\nu(\rho; \theta, \phi)$ that depend parametrically on ρ ,

$$\psi_n(\rho, \theta, \phi) = \sum_{\nu=0}^{\infty} F_{n\nu}(\rho) \Phi_\nu(\rho; \theta, \phi). \quad (4.121)$$

The channel functions Φ_ν are solutions to the hyperangular part of (4.113)

$$\left(\frac{\Lambda^2 + 15/4}{2\mu_3 \rho^2} + V(\rho, \theta, \phi) \right) \Phi_\nu(\rho; \theta, \phi) = U_\nu(\rho) \Phi_\nu(\rho; \theta, \phi), \quad (4.122)$$

and $U_\nu(\rho)$ are the resulting effective potential curves obtained by solving this eigenvalue equation at a number of different hyperradii. Substituting (4.121) into (4.113) and projecting out $\Phi_{\nu'}$ by multiplying the conjugate transpose $\Phi_{\nu'}^\dagger$ to the left and integrating over the hyperangular coordinates results in an infinite set of coupled differential equation in ρ , which reads

$$\begin{aligned} & \left(-\frac{1}{2\mu} \frac{\partial^2}{\partial \rho^2} + U_\mu(\rho) - \frac{1}{2\mu} Q_{\mu\mu}(\rho) \right) F_{n\mu}(\rho) \\ & - \frac{1}{2\mu} \left(\sum_{\nu \neq \mu} 2P_{\mu\nu}(\rho) \frac{\partial}{\partial \rho} + Q_{\mu\nu}(\rho) \right) F_{n\nu}(\rho) = E_n F_{n\mu}(\rho), \end{aligned} \quad (4.123)$$

where the nonadiabatic coupling terms $P_{\mu\nu}$ and $Q_{\mu\nu}$ involve partial first and second derivative of the channel functions with respect to ρ . They are generated by the ρ dependence of the channel functions and are defined as

$$P_{\mu\nu}(\rho) = \left\langle \Phi_\mu \left| \frac{\partial}{\partial \rho} \right| \Phi_\nu \right\rangle, \quad (4.124)$$

and

$$Q_{\mu\nu}(\rho) = \left\langle\left\langle \Phi_\mu \left| \frac{\partial^2}{\partial \rho^2} \right| \Phi_\nu \right\rangle\right\rangle, \quad (4.125)$$

where the double brackets denote integration over the two angular coordinates. Integration by parts, the completeness requirement of the channelfunctions together with the antisymmetric properties of the coupling matrix $P_{\mu\nu}$, i.e. $P_{\mu\nu} = -P_{\nu\mu}$, are used to derive the following relation

$$Q_{\mu\nu} = \frac{dP_{\mu\nu}}{d\rho} + P_{\mu\nu}^2, \quad (4.126)$$

where the square of the coupling matrix $P_{\mu\nu}$ relates to $Q_{\mu\nu}$ through

$$\begin{aligned} P_{\mu\nu}^2 &= \sum_{\sigma} P_{\mu\sigma} P_{\sigma\nu} = \sum_{\sigma} \left\langle\left\langle \Phi_\mu \left| \frac{\partial \Phi_\sigma}{\partial \rho} \right\rangle\right\rangle \left\langle\left\langle \Phi_\sigma \left| \frac{\partial \Phi_\nu}{\partial \rho} \right\rangle\right\rangle \\ &= \sum_{\sigma} -\left\langle\left\langle \frac{\partial \Phi_\mu}{\partial \rho} \left| \Phi_\sigma \right\rangle\right\rangle \left\langle\left\langle \Phi_\sigma \left| \frac{\partial \Phi_\nu}{\partial \rho} \right\rangle\right\rangle = -\left\langle\left\langle \frac{\partial \Phi_\mu}{\partial \rho} \left| \frac{\partial \Phi_\nu}{\partial \rho} \right\rangle\right\rangle. \end{aligned} \quad (4.127)$$

4.4 Generalized Hellmann-Feynman theorem

The following subsection concerns the mathematical description of the non-adiabatic coupling matrices that was defined in subsection 4.3. To obtain an expression for the coupling term $P_{\mu\nu}$ given in (4.124), a generalized Hellmann-Feynman (HF) approach can be used. Consider ν adiabatic eigenstates Φ_ν , which are obtained by

$$H_{ad}\Phi_\nu = U_\nu\Phi_\nu, \quad (4.128)$$

where the adiabatic Hamiltonian H_{ad} is just the hyperangular part of the Schrödinger equation given in (4.122), and the eigenvalues $U_\nu(\rho)$ are the effective adiabatic three-body potential curves. Using the identities

$$\left\langle\left\langle \Phi_\mu \left| \Phi_\nu \right\rangle\right\rangle \equiv \delta_{\mu\nu} \quad (4.129)$$

and

$$\frac{\partial}{\partial \rho} \left\langle\left\langle \Phi_\nu \left| \Phi_\nu \right\rangle\right\rangle \equiv 0, \quad (4.130)$$

we start by deriving the diagonal part of the HF theorem. Projecting Φ_ν out from equation (4.128), and differentiating with respect to the hyperradius gives

$$\begin{aligned}
\frac{\partial U_\nu}{\partial \rho} &= \frac{\partial}{\partial \rho} \langle \Phi_\nu | H_{ad} | \Phi_\nu \rangle \\
&= \langle \Phi_\nu | \frac{\partial H_{ad}}{\partial \rho} | \Phi_\nu \rangle + \langle \Phi_\nu | H_{ad} | \frac{\partial \Phi_\nu}{\partial \rho} \rangle + \langle \frac{\partial \Phi_\nu}{\partial \rho} | H_{ad} | \Phi_\nu \rangle \\
&= \langle \Phi_\nu | \frac{\partial H_{ad}}{\partial \rho} | \Phi_\nu \rangle + U_\nu \langle \Phi_\nu | \frac{\partial \Phi_\nu}{\partial \rho} \rangle + U_\nu \langle \frac{\partial \Phi_\nu}{\partial \rho} | \Phi_\nu \rangle \\
&= \langle \Phi_\nu | \frac{\partial H_{ad}}{\partial \rho} | \Phi_\nu \rangle + U_\nu \frac{\partial}{\partial \rho} \langle \Phi_\nu | \Phi_\nu \rangle \\
&= \langle \Phi_\nu | \frac{\partial H_{ad}}{\partial \rho} | \Phi_\nu \rangle.
\end{aligned} \tag{4.131}$$

The generalized HF theorem also includes the nondiagonal terms. Multiplying with Φ_μ^\dagger to the left of (4.128) and integrating over the two hyperangles, followed by differentiation with respect to the hyperradius gives

$$\begin{aligned}
&\frac{\partial U_\nu}{\partial \rho} \langle \Phi_\mu | \Phi_\nu \rangle + U_\nu \langle \Phi_\mu | \frac{\partial \Phi_\nu}{\partial \rho} \rangle + U_\nu \langle \frac{\partial \Phi_\mu}{\partial \rho} | \Phi_\nu \rangle \\
&= \langle \Phi_\mu | \frac{\partial H_{ad}}{\partial \rho} | \Phi_\nu \rangle + U_\mu \langle \Phi_\mu | \frac{\partial \Phi_\nu}{\partial \rho} \rangle + U_\nu \langle \frac{\partial \Phi_\mu}{\partial \rho} | \Phi_\nu \rangle.
\end{aligned} \tag{4.132}$$

The first term on the left side of this equation is zero by the orthogonality of the channel functions. By removing the last term on both sides we obtain the final expression

$$\langle \Phi_\mu | \frac{\partial H_{ad}}{\partial \rho} | \Phi_\nu \rangle = (U_\nu - U_\mu) \langle \Phi_\mu | \frac{\partial}{\partial \rho} | \Phi_\nu \rangle, \tag{4.133}$$

and we can express the nonadiabatic coupling terms $P_{\mu\nu}$ as

$$P_{\mu\nu} = \frac{1}{(U_\nu - U_\mu)} \langle \Phi_\mu | \frac{\partial H_{ad}}{\partial \rho} | \Phi_\nu \rangle. \tag{4.134}$$

Assume that the channel functions can be expressed as a series of basis functions

$$\Phi_\nu = \sum_j C_\nu^j \varphi_j, \tag{4.135}$$

Where C_ν^j are the expansion coefficients given in TODO(make reference). Anticipating that the Hamiltonian operator will take the matricial form of elements H_{ij} . From the results of the diagonal case discussed in, we obtain the following matricial expression [15]

$$\frac{\partial U_\nu}{\partial \rho} = \sum_{ij} (C_\nu^i)^\dagger C_\nu^j \frac{\partial H_{ij}}{\partial \rho}. \tag{4.136}$$

In the non-diagonal case the result in matricial form reads

$$\left\langle\left\langle\Phi_\mu\left|\frac{\partial}{\partial\rho}\right|\Phi_\nu\right\rangle\right\rangle=P_{\mu\nu}=\sum_{ij}(C_\mu^i)^\dagger C_\nu^j\frac{\partial H_{ij}}{\partial\rho}. \quad (4.137)$$

5 Numerical Approach

We are going to implement a 2D B-spline collocation to solve the adiabatic part of the Hamiltonian given in (4.122). The outline of this method is described in APPENDIX.

The spatial discretization is based on B-spline collocation at Gauss points

5.1 Basis splines expansion

The first step in solving the adiabatic Hamiltonian given by (4.122), is to expand the solution, i.e. the channel functions Φ_ν , in a suitable basis, such as B-splines. For setting up the expansion in the two hyperangular coordinates I followed the description given in [6], which I will describe shortly in the following text. Start by making the ansatz

$$\Phi_\nu(\rho;\theta,\phi)=\sum_{l,m}^{L,M}c_\nu^{l,m}B_{l,k}(\theta)B_{m,k}(\phi). \quad (5.1)$$

The channelfunctions are now characterized by the LM expansion coefficients. The upper limits of this sum is determined by the number of mesh points, the order of the B-splines and the number of conditions (n_c) on the boundaries for the coordinate in question. If we construct a mesh containing N_θ points in the θ -direction and N_ϕ points in the ϕ -direction, then the number of B-splines needed for each coordinate is given by

$$L=N_\theta+k-n_c, \quad (5.2)$$

$$M=N_\phi+k-n_c. \quad (5.3)$$

Boundary conditions are implemented by For a second order partial differential equation the B-splines must be twice differentiable everywhere on the knot sequence and have continuous second order derivatives. With the B-spline definitions given in A, the above requirements is fulfilled for B-splines of order $k \geq 4$. Next, substituting (5.1) into the adiabatic Hamiltonian (4.122) and projecting out $B_{l',k}(\theta)B_{m',k}(\phi)$ gives the matrix equation

$$\mathbf{H}\mathbf{c}=\mathbf{U}\mathbf{B}\mathbf{c}, \quad (5.4)$$

where \mathbf{c} is the column vector with the coefficients $c_\nu^{l,m}$. Mapping the two indices l and m into a single index i gives

$$i=(l-1)M+m. \quad (5.5)$$

The matrix elements of the Hamiltonian now reads

$$H_{i'i} = \iint d\theta d\phi B_{l',k}(\theta) B_{m',k}(\phi) H_{ad}(\rho; \theta, \phi) B_{l,k}(\theta) B_{m,k}(\phi), \quad (5.6)$$

and the overlap matrix elements are given by

$$B_{i'i} = \iint d\theta d\phi B_{l',k}(\theta) B_{m',k}(\phi) B_{l,k}(\theta) B_{m,k}(\phi). \quad (5.7)$$

The potential term in the adiabatic Hamiltonian cannot be separated into a product of two one-dimensional integral and must thus be integrated in two angular dimensions. Since the basis functions used in the expansion are B-splines, which are piecewise polynomial functions of degree $k - 1$, the overlap matrix and the kinetic terms in the Hamiltonian can be evaluated exactly, within machine epsilon, using Gauss-Legendre quadrature.

5.2 Gauss-Legendre Quadrature

All integrals are calculated with Gaussian quadrature. A k -point Gaussian quadrature rule is constructed to give an exact result for polynomials of degree $2k - 1$ or less by a suitable choice of the abscissas

$$\begin{aligned} & \int_{t_i}^{t_{i+1}} \int_{u_i}^{u_{i+1}} d\theta d\phi B_{l',k}(\theta) B_{m',k}(\phi) f(\theta, \phi) B_{l,k}(\theta) B_{m,k}(\phi) \\ &= \sum_{n=1}^k \sum_{p=1}^k w_n w_p B_{l',k}(\theta_n) B_{m',k}(\phi_p) f(\theta_n, \phi_p) B_{l,k}(\theta_n) B_{m,k}(\phi_p) \end{aligned} \quad (5.8)$$

6 Results

N_θ	λ_{00}	λ_{13}	λ_{26}	array(s)	dsygvd(s)
5	0.000 000 000 0214	32.000 000 071 3015	60.000 002 031 0135	0.66	0.00
10	-0.000 000 000 0417	32.000 000 000 1003	60.000 000 000 2154	4.58	0.00
15	0.000 000 000 0007	32.000 000 000 1309	59.999 999 999 8871	12.32	0.02

Table 2: Analytically derived eigenvalues

A Basis splines

A basis spline, or B-spline, of order k is a piecewise polynomial function of degree $(k - 1)$ defined on a collection of points, t_i , called *knotpoints*. The array formed by these knotpoints are referred to as *knot sequence*, or knot vector, where

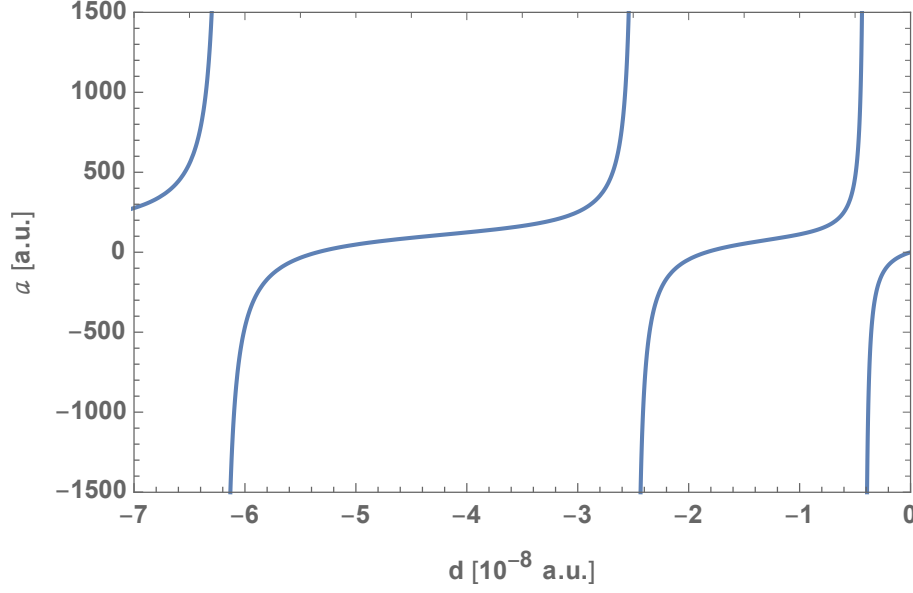


Figure 6.1: Adiabatic potential curves U_ν as a function of the hyperradius ρ for $a = 228$.

$t_i \leq t_{i+1}$. B-splines of order k can be defined recursively by the Cox-de Boor formula. With a given knot sequence, the B-splines of order $k = 1$ is defined as

$$B_{i,k=1}(x) \doteq \begin{cases} 1, & \text{if } t_i \leq x < t_{i+1} \\ 0, & \text{otherwise} \end{cases} \quad (\text{A.1})$$

and if $k > 1$

$$B_{i,k}(x) \doteq \frac{x - t_i}{t_{i+k-1} - t_i} B_{i,k-1}(x) + \frac{t_{i+k} - x}{t_{i+k} - t_{i+1}} B_{i+1,k-1}(x). \quad (\text{A.2})$$

The B-splines are local in the sense that they will be non-zero only in a limited region of space. If the numbering is such that the first knot point is t_1 and the first B-spline is $B_{1,k}$, then the B-spline $B_{i,k}$ is non-zero within the region $t_i \leq x \leq t_{i+k}$. On a given knot sequence (t_1, \dots, t_N) the B-splines form a complete set

$$\sum_{i=1}^N B_{i,k}(x_i) = 1. \quad (\text{A.3})$$

By placing $(k - 1)$ additional points, called ghost points, at the endpoints, the B-splines will be confined within the region $t_1 \leq x \leq t_N, (k - 1)$. This means that N knot points in one dimension correspond to $N - 2(k - 1)$ physical points

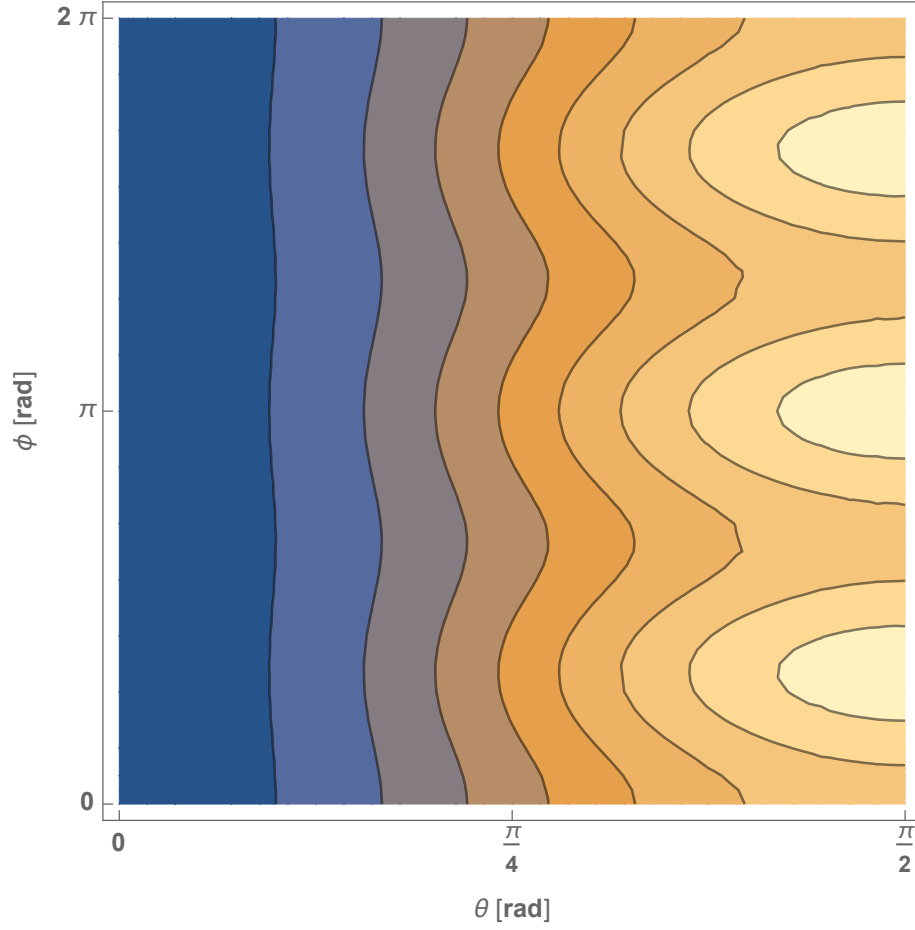


Figure 6.2: Adiabatic potential curves U_ν as a function of the hyperradius ρ for $a = 228$.

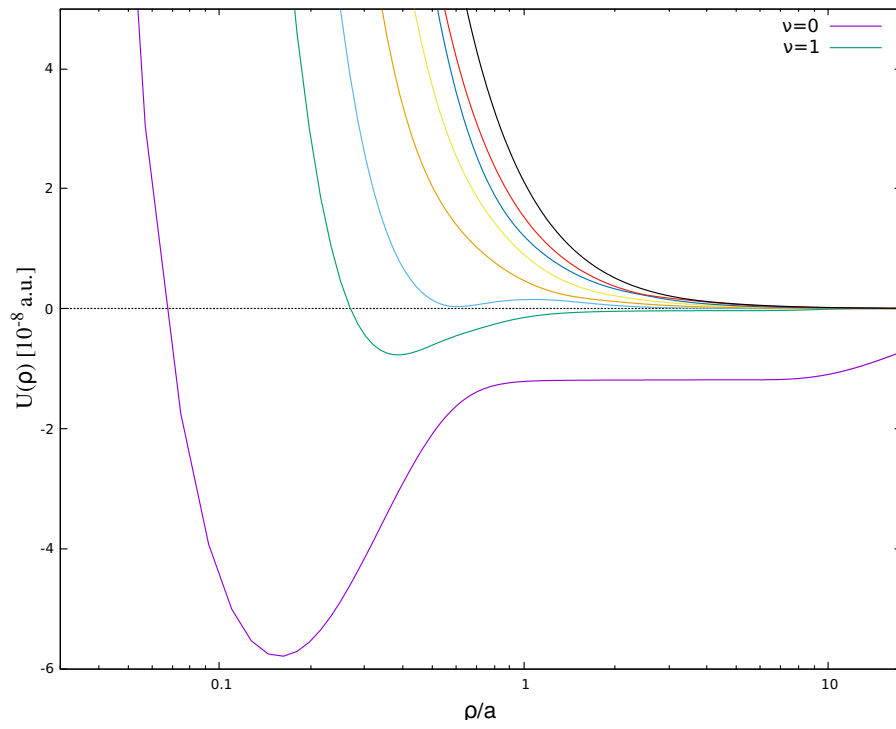


Figure 6.3: Adiabatic potential curves U_v as a function of the hyperradius ρ for $a = 228$.

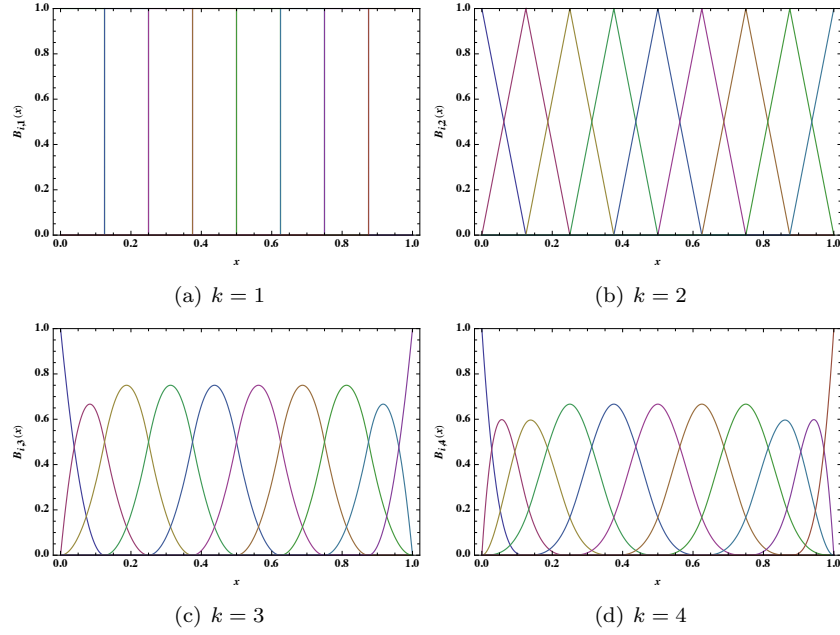


Figure A.1: The subfigures above show the B-splines $B_{i,k}(x)$ of different orders k on a one dimensional mesh.

in that coordinate dimension. This is a common choice because consequentially, this makes only the first B-spline non-zero at the first physical point.

The first derivative of a B-spline of order k is given by

$$\frac{\partial}{\partial x} B_{i,k}(x) = (k-1) \left(\frac{B_{i,k-1}(x)}{t_{i+k-1} - t_i} + \frac{B_{i+1,k-1}(x)}{t_{i+k} - t_{i+1}} \right), \quad (\text{A.4})$$

and the second derivative

$$\begin{aligned} \frac{\partial^2}{\partial x^2} B_{i,k}(x) = & \frac{(k-1)(k-2)B_{i,k-2}(x)}{(t_{i+k-1} - t_i)(t_{i+k-2} - t_i)} - \frac{(k-1)(k-2)B_{i+1,k-2}(x)}{(t_{i+k-1} - t_i)(t_{i+k-1} - t_{i+1})} \\ & - \frac{(k-1)(k-2)B_{i+1,k-2}(x)}{(t_{i+k} - t_{i+1})(t_{i+k-1} - t_{i+1})} + \frac{(k-1)(k-2)B_{i+2,k-2}(x)}{(t_{i+k} - t_{i+1})(t_{i+k} - t_{i+2})}. \end{aligned} \quad (\text{A.5})$$

B-splines can be used to form basis functions.

$$f(x_i) = \sum_{n=i-k+1}^{i-1} c_n B_{n,k}(x_i). \quad (\text{A.6})$$

References

- [1] Kajsa-My Blomdahl. “Numerical Calculations of Efimov States in Ultracold Atomic Systems”. MA thesis. <http://www.diva-portal.org>; KTH, 2016.
- [2] Eric Braaten, Masaoki Kusunoki, and Dongqing Zhang. “Scattering models for ultracold atoms”. In: *Annals of Physics* 323 (July 2008), pp. 1770–1815. DOI: 10.1016/j.aop.2007.12.004. arXiv: 0709.0499 [cond-mat.other].
- [3] Alain Chenciner. “Poincaré and the Three-Body Problem”. In: *Henri Poincaré, 1912–2012: Poincaré Seminar 2012*. Ed. by Bertrand Duplantier and Vincent Rivasseau. Basel: Springer Basel, 2015, pp. 51–149. ISBN: 978-3-0348-0834-7. DOI: 10.1007/978-3-0348-0834-7_2. URL: https://doi.org/10.1007/978-3-0348-0834-7_2.
- [4] V. Efimov. “Energy levels arising from the resonant two-body forces in a three-body system”. In: *Phys. Lett.* 33B (1970), pp. 563–564. DOI: 10.1016/0370-2693(70)90349-7.
- [5] Vitaly Efimov. “Is a qualitative approach to the three-body problem useful?” In: *Comments Nucl. Part. Phys.* 19 (1990), pp. 271–293.
- [6] Brett Esry. “MANY-BODY EFFECTS IN BOSE-EINSTEIN CONDENSATES OF DILUTE ATOMIC GASES”. PhD thesis. University of Colorado, 1997.
- [7] L. D. Faddeev. “Scattering theory for a three particle system”. In: *Sov. Phys. JETP* 12 (1961). [Zh. Eksp. Teor. Fiz.39,1459(1960)], pp. 1014–1019.
- [8] Francesca Ferlaino et al. “Evidence for Universal Four-Body States Tied to an Efimov Trimer”. In: *Physical review letters* 102 (May 2009), p. 140401. DOI: 10.1103/PHYSREVLETT.102.140401.
- [9] Bo Huang et al. “Observation of the Second Triatomic Resonance in Efimov’s Scenario”. In: *Phys. Rev. Lett.* 112 (19 May 2014), p. 190401. DOI: 10.1103/PhysRevLett.112.190401. URL: <https://link.aps.org/doi/10.1103/PhysRevLett.112.190401>.
- [10] B. R. Johnson. “On hyperspherical coordinates and mapping the internal configurations of a three body system”. In: *The Journal of Chemical Physics* 73.10 (1980), pp. 5051–5058. DOI: 10.1063/1.439983. eprint: <https://doi.org/10.1063/1.439983>. URL: <https://doi.org/10.1063/1.439983>.
- [11] T. Kraemer et al. “Evidence for Efimov quantum states in an ultracold gas of caesium atoms”. In: *Nature* 440 (Mar. 2006), URL: <http://dx.doi.org/10.1038/nature04626>.
- [12] Maksim Kunitski et al. “Observation of the Efimov state of the helium trimer”. In: *Science* 348 (2015), pp. 551–555. DOI: 10.1126/science.aaa5601. arXiv: 1512.02036 [physics.atm-clus].

- [13] L. D. Landau and L. M. Lifshitz. *Quantum Mechanics Non-Relativistic Theory, Second Edition: Volume 3*. 2nd ed. Pergamon Press, 1965. ISBN: 0750635398.
- [14] H R Sadeghpour et al. “Collisions near threshold in atomic and molecular physics”. In: *Journal of Physics B: Atomic, Molecular and Optical Physics* 33.5 (Feb. 2000), R93–R140. DOI: 10.1088/0953-4075/33/5/201. URL: <https://www.cfa.harvard.edu/~hrs/PubList/JPBThresholdReviw2000.pdf><https://doi.org/10.1088/0953-4075/33/5/201>.
- [15] Cristina Sanz-Sanz et al. “Non-adiabatic couplings and dynamics in proton transfer reactions of H_n^+ systems: Application to $H_2^+ + H_2 \rightarrow H + H_3^+$ collisions”. In: *The Journal of Chemical Physics* 143.23 (2015), p. 234303. DOI: 10.1063/1.4937138. eprint: <https://doi.org/10.1063/1.4937138>. URL: <https://doi.org/10.1063/1.4937138>.
- [16] Felix T. Smith. “A Symmetric Representation for Three Body Problems. I. Motion in a Plane”. In: *Journal of Mathematical Physics* 3.4 (1962), pp. 735–748. DOI: 10.1063/1.1724275. eprint: <https://doi.org/10.1063/1.1724275>. URL: <https://doi.org/10.1063/1.1724275>.
- [17] Alexander L. Zubarev and Victor B. Mandelzweig. “Exact solution of the four-body Faddeev-Yakubovsky equations for the harmonic oscillator”. In: *Phys. Rev. C* 50 (1 July 1994), pp. 38–47. DOI: 10.1103/PhysRevC.50.38. URL: <https://link.aps.org/doi/10.1103/PhysRevC.50.38>.